Journal of Medicinal Chemistry

Article

pubs.acs.org/jmc

Synthesis and Structure−Activity Relationship of 3-Hydroxypyridine-2-thione-Based Histone Deacetylase Inhibitors

Quaovi H. Sodji,[†,∥] Vishal Patil,[†,∥] James R. Kornacki,[§,∥] Milan Mrksich,*[,§] and Adegboyega K. Oyelere*[,†,‡]

[†]School of Chemistry and Biochemistry, [‡]Parker H. Petit Institute for Bioengineering and Bioscience, Georgia Institute of Technology, Atlanta, Georgia 30332-0400, United States

[§]Departments of Chemistry and Biomedical Engineering, Northwestern University, 2145 Sheridan Road, Evanston, Illinois 60208-3113, United States

Supporting Information

ABSTRACT: We previously identified 3-hydroxypyridine-2-thione (3HPT) as a novel zinc binding group for histone deacetylase (HDAC) inhibition. Early structure−activity relationship (SAR) studies led to various small molecules possessing selective inhibitory activity against HDAC6 or HDAC8 but devoid of HDAC1 inhibition. To delineate further the depth of the SAR of 3HPT-derived HDAC inhibitors (HDACi), we have extended the SAR studies to include the linker region and the surface recognition group to optimize the HDAC inhibition. The current efforts resulted in the identification of two lead compounds, **10d** and **14e**, with potent HDAC6 and HDAC8 activities that are inactive against HDAC1. These new HDACi possess anticancer activities against various cancer cell lines including Jurkat J.γ1 for which SAHA and the previously disclosed 3HPT-derived HDACi were inactive.

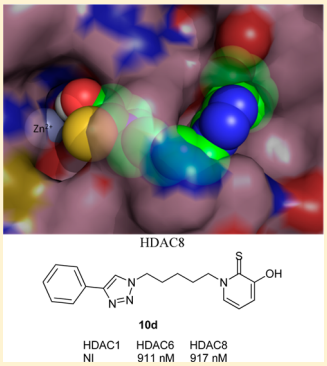

INTRODUCTION

Histone deacetylase (HDAC) inhibition is a promising epigenetic strategy for cancer treatment, and several distinct small-molecule histone deacetylase inhibitors (HDACi) have been reported.[1] Currently, two of these HDACi, suberoylanilide hydroxamic acid (SAHA) (Figure 1) and cyclic peptide FK228 (Romidepsin), are approved for the treatment of cutaneous T-cell lymphoma (CTCL).[2] However, most HDACi, including the clinically approved agents, nonselectively inhibit the deacetylase activity of class I and II HDACs, and many suffer from metabolic instability. These shortcomings have been associated with reduced in vivo potency and toxic side effects.[3] Currently, significant efforts are ongoing to address these and other deficiencies of HDACi to bolster the potential of HDAC inhibition in cancer treatment.

Most HDACi fit a three-motif pharmacophoric model consisting of a zinc binding group (ZBG), a linker, and a surface recognition cap group. Hydroxamic acid (hydroxamate) is by far the most common ZBG moiety in HDACi owing to its ability to reliably chelate active-site zinc ions.[4] However, pharmacodynamic and pharmacokinetic liabilities of the hydroxamate moiety have prompted efforts to find better-suited alternatives.[5] Examples of nonhydroxamate ZBGs investigated include thiols, α-ketoesters, benzamide, trifluoromethylketone, oxime, phosphonates, and mercaptoacetamide.[6,7,5,8] However, most of these alternative ZBGs have thus far elicited reduced potency relative to hydroxamic acid.

Previous work from our lab has established 3-hydroxypyridine-2-thione (3HPT) as a nonhydroxamate ZBG for HDAC inhibition.[9] Initial structure−activity relationship (SAR) studies led to aryl- and diaryl-3HPT analogues possessing selective inhibitory activity against HDAC6 or HDAC8 but not against HDAC1 (Figure 1, representative compounds **1**, **2**, and **3**). In the same study, we observed that the replacement of the proximal phenyl ring of the lead biphenyl compound **2** with a 1,2,3-triazole ring resulted in corresponding triazolyl analogue **3** lacking HDAC6 inhibition activity but having improved HDAC8 inhibition (Figure 1). This observation suggests a possible divergence in the SARs of the triazole and biphenyl 3-HPT compounds.[9] To characterize such divergence further, we have expanded the SAR studies on the 3-HPT compounds bearing triazole-linked cap groups. The current efforts identified two lead compounds, **10d** and **14e**, which are potent inhibitors of HDAC6 and HDAC8 but are inactive against HDAC1. These new HDACi possess anticancer activities against various cancer cell lines including Jurkat J.γ1 against which SAHA and the previously disclosed 3HPT-derived HDACi were inactive.

RESULTS AND DISCUSSION

SAR on the Linker Moiety. The hydrophobic linker moiety of most HDACi consists of flexible methylene spacer groups that separate the ZBG from the cap group to tailor the

Received: August 7, 2013
Published: December 4, 2013

   dx.doi.org/10.1021/jm401225q | J. Med. Chem. 2013, 56, 9969−9981

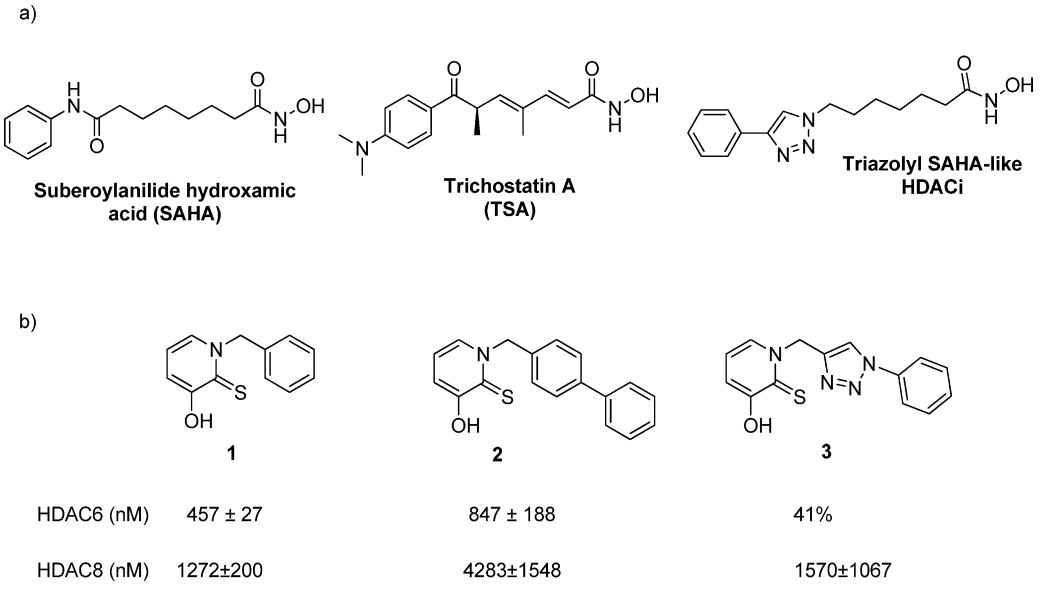

Figure 1. (a) Representative examples of HDACi. (b) Representative aryl- and diaryl-3HPT-based HDACi with their HDAC inhibition activities (IC_{50}). For compound **3**, the percent inhibition of at 10 μM is shown.[9]

Scheme 1. Synthesis of 3-HPT-Based HDACi 10 for SAR Studies[a]

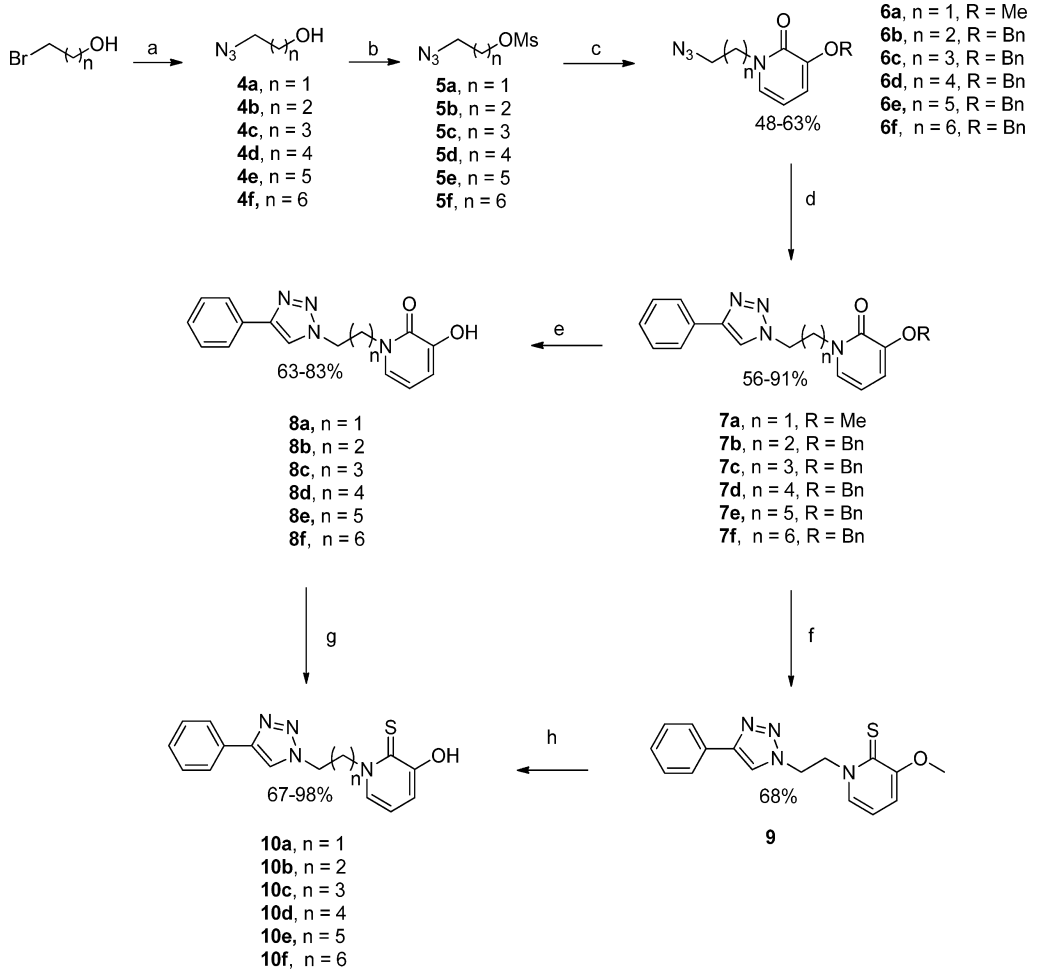

[a]Conditions: (a) NaN_3, DMF, 75 °C; (b) methanesulfonyl chloride, Et_3N, THF; (c) 3-methoxypyridin-2-one or 3-benzyloxypyridin-2-one, K_2CO_3, THF/DMF, reflux; (d) phenylacetylene, CuI, DIPEA, THF; (e) H_2, Pd/C, THF for R = Bn and BBr_3, DCM for R = Me; (f) for **7a** only: Lawesson's reagent, toluene, reflux; (g) P_4S_{10}, 175 °C, neat; (h) BBr_3, DCM.

dx.doi.org/10.1021/jm401225q | J. Med. Chem. 2013, 56, 9969−9981

Table 1. SAR on Linker of Triazolic Compounds

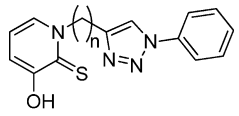

n = 1, 2, 3, 4, 5, 6, 7

compound	*n*	HDAC1 IC_{50} (nM)	HDAC6 IC_{50} (nM)	HDAC8 IC_{50} (nM)
3a	1	NI[a]	41%[b]	1570 ± 1067
10a	2	NI	14%	6050 ± 750
10b	3	NI	3628 ± 1363	6400 ± 450
10c	4	NI	1085 ± 333	3303 ± 260
10d	5	NI	911 ± 173	917 ± 139
10e	6	NI	22%	6751 ± 910
10f	7	NI	955 ± 150	1377 ± 205
SAHA		38 ± 2	144 ± 23	232 ± 19

[a]No significant inhibition (below 20% inhibition at 10 μM). [b]Percent inhibition of the compounds at 10 μM are given if the IC_{50} was above 10 μM.

intramolecular span between the active-site Zn^{2+} ion and outer-rim amino acid residues. Previous studies from our laboratory have shown that SAHA-like HDACi containing a 1,2,3-triazole ring within the linker region differentially inhibited HDACs as a function of linker length.[10] Lead compound **3** is an analogue with one methylene spacer separating the triazole ring and the 3HPT ZBG. To probe the effect of the spacer length on HDAC inhibition activity, we initially synthesized and investigated the anti-HDAC activity of compounds **10a−f**, analogues of **3** with increasing methylene groups. The syntheses of target compounds were accomplished as shown in Scheme 1. The reaction of various bromoalkanols with sodium azide yielded their corresponding azidoalkanols, **4a−f**. Subsequent mesylation of **4a−f** followed by N-alkylation with *O*-methyl-or *O*-benzyl-protected 3-hydroxypyridin-2-one (3HP) gave the azido intermediates **6a−f**. The phenyl moiety, which serves as surface recognition group, was introduced via Cu(I)-catalyzed Huisgen cycloaddition reaction[11,12] between phenylacetylene and azido intermediates **6a−f** to afford compounds **7a−f**. The deprotection of the *O*-benzyl moiety of **7b−f** was accomplished using catalytic hydrogenation to afford compounds **8b−f**, which, upon treatment with P_4S_{10} at 175 °C, gave corresponding 3HPT compounds **10b−f** (Scheme 1).[13] Although otherwise facile, this chemistry did not work for the two methylene linker compound because of an extensive degradation that resulted in an intractable mixture when compound **8a** was exposed to P_4S_{10} at 175 °C. To obtain the requisite 3HPT compound **10a**, *O*-methyl protected 3HP **7a** was first converted to its thione analogue, **9**, using Lawesson's reagent.[14] Subsequent BBr_3 deprotection of the methyl ether group yielded desired compound **10a** (Scheme 1).

We then assayed compounds **10a−f** as well as their 3HP congeners, **8a−f**, against HDAC isoforms 1, 6 and 8 using SAMDI mass spectrometry as previously described.[15−17] 3HP compounds **8a−f** are inactive against all HDAC isoforms tested (data not shown), a result that is in agreement with our previous observation on aryl- and diaryl-3HP analogues.[9] As previously reported for diaryl-3HPT-based HDACi, compounds **10a−f** are not active against HDAC1. However, compounds **10a−f** do inhibit HDAC6 and HDAC8 (Table 1), and they do so as a function of methylene linker length. Such apparent selectivity may result from active-site structure differences between the isoforms. The channel to HDAC1 active site is narrow as opposed to HDAC6 whose hydrophobic channel entrance appears large enough to accommodate the 3HPT group.[18] Relative to lead compound **3**, a progressive increase in the length of the methylene linker separating the triazole ring and the 3HPT group results in a corresponding increase in HDAC6 inhibition activity up to five methylene units (n = 5) (Table 1, compare **10a−d**). A single methylene linker extension (from n = 5 to 6) is not tolerated, as resulting analogue **10f** is devoid of HDAC6 inhibition activity; however, a further extension of the methylene linker length (n = 7) fully restores anti-HDAC6 activity (Table 1, compare **10d−f**). Similar methylene-linker-length-dependence in HDAC8 inhibition activity was observed. However, unlike what was obtained with HDAC6, no complete loss and subsequent full restoration of anti-HDAC8 occurred when n = 6 and 7, respectively. This initial SAR study suggests that five methylene spacers (n = 5) are optimum for HDAC inhibition, as corresponding compound **10d** is the most potent in this series, with a markedly improved anti-HDAC activity relative to starting lead compound **3**. Additionally, **10d** is equipotent against HDAC6 and HDAC8 with an IC_{50} of approximately 900 nM (Table 1).

Molecular Docking Analyses. To understand the structural basis of dependence of methylene linker length on the HDAC inhibition by compounds **10a−f**, we docked selected analogues (**10a** and **10d**) against an HDAC6 homology model built from HDAC8 (PDB code: 3F0R) and HDAC8 (PDB code: 3SFF) using AutoDock 4.2.[15,19,20] We observed that **10a** and **10d** adopt docked conformations on HDAC6 such that their 3HPT ZBG are able to maintain Zn^{2+} chelation irrespective of the methylene linker length. Unlike **10a**, however, five methylene compound **10d** is further stabilized by a π-stacking interaction between its phenyl ring and that of Phe680 (Figure 2A). The docked poses found on HDAC8 have the phenyl ring of **10d** inserted into a solvent-inaccessible hydrophobic pocket adjacent to the active site that is otherwise inaccessible to **10a** because of its shorter methylene spacers. Instead, the phenyl ring of **10a** is positioned in a solvent-exposed outer-rim compartment of HDAC8 (Figure 2B). The favorable interactions of the phenyl ring with the active-site amino acid side chains of HDAC6 and the subpocket of HDAC8 support the preference for five methylene compound **10d**.

SAR on the Surface Recognition Group: Optimization of the Five Methylene-Linked Compound. As demonstrated by in vitro studies and corroborated by docking analyses, the five methylene spacer groups induced optimal inhibition of both HDAC6 and HDAC8. This linker, along with

dx.doi.org/10.1021/jm401225q | J. Med. Chem. 2013, 56, 9969−9981

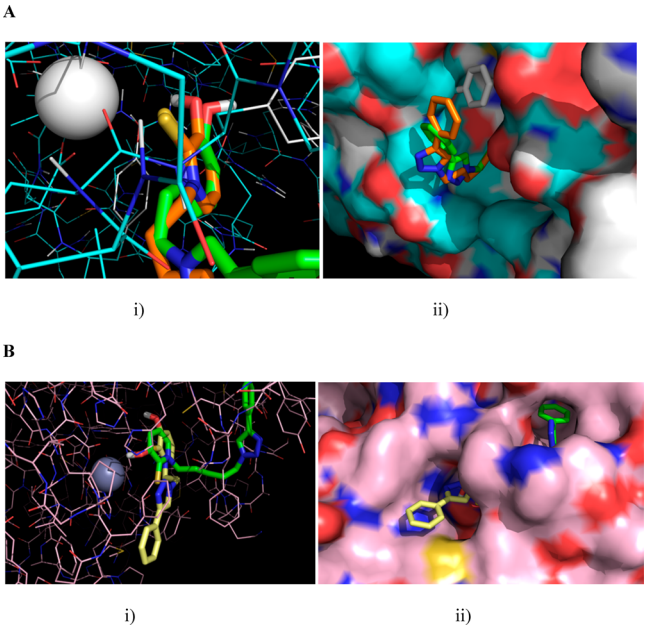

Figure 2. Molecular docking studies on **10a** and **10d**. (A) HDAC6 homology model built from HDAC8 (PDB code: 3F0R). (i) Zn^{2+} chelation is observed for both **10a** (green) and **10d** (orange). (ii) π-Stacking interaction of the phenyl ring of **10d** with Phe680. (B) HDAC8 (PDB code: 3SFF). (i) Zn^{2+} chelation of **10a** (yellow) and **10d** (green). (ii) The phenyl ring of **10d** (green) is inserted into a hydrophobic pocket adjacent to the active site, whereas that of **10a** (yellow) is in a solvent-exposed HDAC8 outer rim.

the triazole ring, traverses the hydrophobic channel of the HDAC to present the 3-HPT to the active site for Zn^{2+} chelation. To optimize lead compound **10d** further, we performed a SAR study on the cap group by investigating the effects of various phenyl-ring substituents and substitution patterns on HDAC inhibition activity.

The synthesis of the desired phenyl-substituted compounds followed a similar protocol as that described for the synthesis of compound **10** (Scheme 2). Briefly, Cu(I)-catalyzed Huisgen cycloaddition reaction[11,12] of appropriately substituted phenylacetylene with azido *O*-methyl-protected 3-hydroxypyridin-2-one **11** gave corresponding triazolyl intermediates **12a–g**. Subsequent treatment of **12a–g** with Lawessons' reagent followed by BBr_3 deprotection of the *O*-methyl group resulted in desired 3HPT compounds **14a–g**. Similarly, BBr_3 deprotection of the *O*-methyl group of **12a–g** afforded corresponding 3HP compounds **15a–g**.

As expected, 3HP compounds **15a–g** were inactive against all HDAC isoforms tested (data not shown). Similar to 3HPT compounds **10a–f**, none of substituted 3HPT compounds **14a–g** were active against HDAC1. Despite the diversity of the surface recognition groups tested, none was more potent than unsubstituted lead compound **10d** against HDAC8 (Table 2). Against HDAC6, however, we observed an intriguing effect on inhibition activity. Among the methyl substituents (*para* **14a**, *meta* **14b**, and *ortho* **14c**), only ortho-substituted **14c** offered a potency enhancement against HDAC6 relative to **10d**. The inhibitory activity of para-substituted compound **14a** is comparable to that of **10d**, whereas meta-substituted compound **14b** is somewhat less potent. Remarkably, substitution of methyl at the meta position of **14b** with an electron-withdrawing cyano group yielded the most potent HDAC6 inhibitor, compound **14e**, among the series. Compound **14e** is 2.5- and 3-fold more effective than unsubstituted lead compound **10d** and meta-methyl compound **14b**, respectively (Table 2). The placement of the cyano group at the para position conferred no additional benefit to HDAC inhibitory activity, as resulting compound **14d** is equipotent as lead compound **10d** and para-methyl compound **14a**. Moreover, switching to the electron-donating *N*,*N*-dimethylamino group at the para position (compound **14f**) did not enhance HDAC6 inhibition despite structural similarity to TSA. Addition of a different electron-withdrawing group, a trifluoromethyl moiety, to the meta position in the presence of the cyano substituent at the para position partially rescued the HDAC6 inhibitory activity that was lost in the compound that has only the cyano group at the para position (Table 2, compare **14d** and **14g**). This observation further supports the influence of electron-withdrawing groups at the meta position on the potency of the substituted 3-HPT compounds.

Molecular Docking Analysis on Substituted 3HPT Compounds. To gain insight into the binding interactions

Scheme 2. Optimization of the Surface Recognition Group: Synthesis of the Five Methylene-Linked 3HPT HDACi[a]

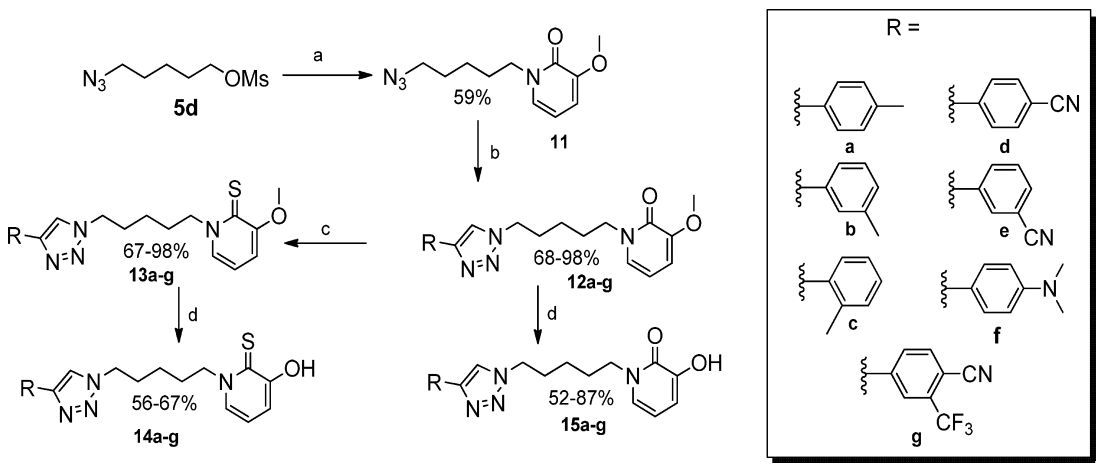

[a](a) 3-Methoxypyridin-2-one, K_2CO_3, THF/MeOH, reflux; (b) substituted phenylacetylenes (**a–g**), CuI, DIPEA, DMSO/THF; (c) Lawesson's reagent, toluene, reflux; d) BBr_3, DCM.

dx.doi.org/10.1021/jm401225q | J. Med. Chem. 2013, 56, 9969–9981

Table 2. HDAC Inhibition Profile of the Substituted 3HPT Compounds

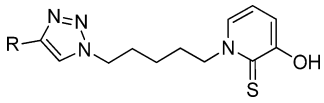

Compound	R	HDAC1 IC_{50} (nM)	HDAC6 IC_{50} (nM)	HDAC8 IC_{50} (nM)
10d	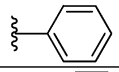	NI[a]	911 ± 173	917 ± 139
14a	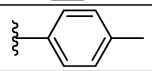	NI	807 ± 207	2533 ± 823
14b	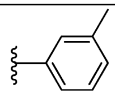	NI	1100 ± 443	1660 ± 416
14c	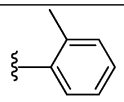	NI	637 ± 160	2402 ± 263
14d	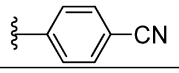	NI	905 ± 249	1465 ± 217
14e	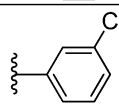	NI	356 ± 72	2831 ± 520
14f	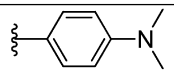	NI	1006 ± 425	1482 ± 389
14g	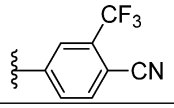	NI	661 ± 121	2258 ± 1005
SAHA	-	38 ± 2	144 ± 23	232 ± 19

[a]No significant inhibition (below 20% inhibition at 10 μM concentration)).

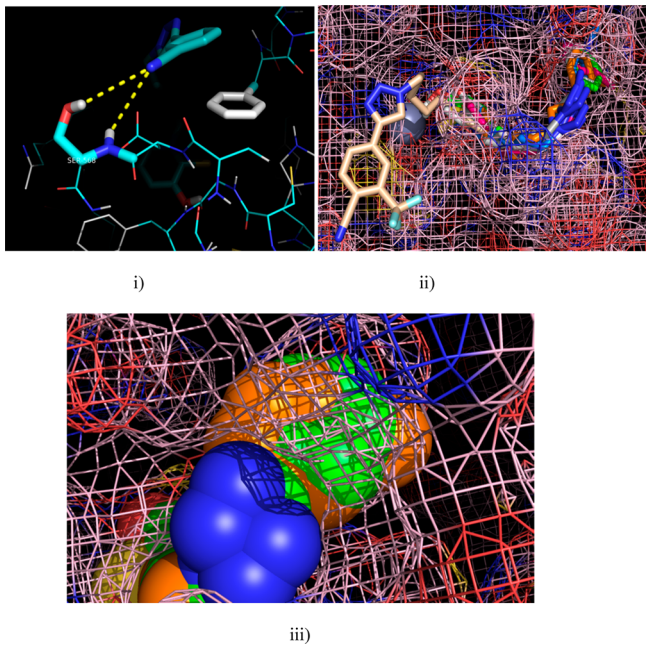

Figure 3. Molecular docking studies on substituted 3HPT compounds. (i) HDAC6 homology model built from HDAC8 (PDB code: 3F0R). The cyano group of compound **14e** is positioned for potential H-bonding interactions with the hydroxyl side chain and amide backbone of Ser568. (ii) HDAC8 (PDB code: 3SFF). The cap groups of monosubstituted compounds are inserted within HDAC8 subpocket, whereas that of disubstituted compound **14g** is excluded. (iii) HDAC8. Space-filling model reveals a better fit of unsubstituted phenyl **10d** (green) within the HDAC8 subpocket relative to representative monosubstituted compound **14b** (orange).

that underlie the SAR for HDAC inhibition, we docked each of the substituted 3HPT compounds against our HDAC6 homology model and HDAC8. For HDAC6, the phenyl ring of all compounds mediates a potential π-stacking interaction with the phenyl ring of Phe680, mimicking the interaction observed for compound **10d** (see Supporting Information Figure S1). Most striking, however, is the observation that the cyano group of compound **14e** is ideally positioned for a stabilizing H-bonding interaction with the hydroxyl side chain and amide backbone of Ser568 and likely accounts for its enhanced potency against HDAC6 (Figure 3). Moreover, the concomitant reduction in electron density by the cyano group could further enhance the stacking interaction with the phenyl ring of Phe680.

Although phenyl ring substitution impaired HDAC8 inhibition, docking analyses offered useful insight into the putative hydrophobic pocket in which the inhibitor's phenyl group is expected to reside. Monosubstituted compounds fit within this subpocket, whereas disubstituted compound **14g** is excluded, indicating a restrictive size limitation (Figure 3 and Supporting Information Figure S2). Space-filling models of all of the docked compounds reveal that unsubstituted phenyl **10d** fit in the subpocket the best and that any substituent slightly pushes the phenyl ring out of the hydrophobic pocket (Figure 3). Even though the size limitation may preclude the subpocket from affecting enhanced inhibition through lead development, it offers a distinctive feature not observed on HDAC6 that accounts for the pronounced isoform selectivity of compound **14e.** The lead candidates from the foregoing SAR studies are compounds **10d** and **14e**. Compound **10d** is equipotent against HDAC6 and HDAC8, whereas **14e** is 8-fold-selective for HDAC6.

In Vitro Cell Growth Inhibition. We next tested the effect of lead compounds **10d** and **14e** and comparable compounds **10f** and **14c** on the proliferation of selected cancer cell lines. We investigated DU-145 (androgen-independent prostate cancer), LNCaP (androgen-dependent prostate cancer), Jurkat (T-cell leukemia cell line), and Jurkat J.γ1 (a mutant Jurkat cell line resistant to HDAC inhibition).[9,21]

Table 3 shows the IC_{50} values of each compound against the cancer cell lines studied. Lead meta-cyano compound **14e** is about 2-fold more potent against DU145 and LNCaP prostate cancer cell lines relative to unsubstituted congener **10d**. Such improved sensitivity with **14e** toward prostate cancer lines, particularly LNCaP, may be rationalized by its HDAC6 selectivity.[22] LNCaP is an androgen-dependent prostate cancer line whose viability is linked to the interaction between HSP90 and its client proteins including the androgen receptor.[23] Misregulation of HSP90−client protein interactions following HDAC6 inhibition is detrimental to cell viability.[22] Inhibition of HSP90 has been shown to compromise the viability of DU145, offering a similar rationale for the enhanced cytotoxicity of **10d** against this cell line.[24,25] Compounds **10d** and **14e** are equipotent against the wild-type Jurkat cell line

dx.doi.org/10.1021/jm401225q | J. Med. Chem. 2013, 56, 9969−9981

Table 3. Cell Viability Assay[a]

compound	cellular IC_{50} (μM)				
	DU-145	LNCaP	Jurkat	Jurkat J.γ1	Vero
10d	9.33 ± 0.96	5.43 ± 0.47	3.27 ± 0.60	1.86 ± 0.21	>20
10f	17.72 ± 3.28	10.95 ± 1.92	9.04 ± 1.31	>20	NT[b]
14c	11.08 ± 2.38	4.95 ± 0.43	5.18 ± 1.18	NT	NT
14e	5.03 ± 1.13	3.49 ± 0.34	3.44 ± 0.57	0.90 ± 0.12	>20
SAHA	2.49 ± 0.2	2.31 ± 0.74	1.49 ± 0.10	NI[c]	5.20 ± 0.96[d]
Tubastatin A	NT	10.88 ± 1.49	3.38 ± 0.26	NI	>20

[a]IC_{50} of selected compounds against various cancer cell lines. [b]NT, not tested. [c]NI, no inhibition at 20 μM. [d]Ref 15.

despite the enhanced HDAC8 inhibition activity of the former (Table 2), which was expected to favor cytotoxicity to the Jurkat cell line.[21,26] It is reasonable that the compensation of the weaker HDAC8 inhibition activity of **14e** by the 3-fold increase in its anti-HDAC6 activity, relative to that of **10d**, may contribute to its cytotoxicity in the Jurkat cell. The cytotoxicity of **10f**, an analogue containing a seven methylene linker, and ortho-methyl-substituted five methylene compound **14c** do not completely trend with the pattern of their HDAC inhibition activities. Against both prostate cancer lines investigated, **10f** is 2- and 3-fold less cytotoxic compared with lead compounds **10d** and **14e**, respectively, whereas it is 3-fold less cytotoxic relative to both lead compounds against the wild-type Jurkat cell line. Ortho-substituted compound **14c** is 2-fold less cytotoxic against DU145, whereas it is only marginally less cytotoxic against LNCaP and the wild-type Jurkat cell line compared with **14e**.

Although **10d** and **10f** have similar IC_{50} against HDAC6, the latter has a significantly higher cellular IC_{50} against LNCaP cells. Against the Jurkat cell line, **14c** and **14e** also display similar incongruity, which we first attributed to solubility differences. To account partially for such pharmacokinetic liabilities, we estimated the solubility of each tested compound,[27,28] but we found that the four compounds had solubilities greater than the threshold proposed to affect cell activity adversely (Supporting Information, Figure S3 and Table S1). This suggests that the observed discrepancies may be attributed to factors other than solubility.

We have shown previously that the Jurkat J.γ1 cell line, a mutant Jurkat cell line lacking phospholipase C activity, is resistant to SAHA.[9] To check if the 3HPT compounds would be similarly innocuous, we investigated the effect of lead compounds **10d**, **10f**, and **14e** on Jurkat J.γ1 cell growth. We observed that compound **10f** is significantly less cytotoxic to Jurkat J.γ1 cells versus their wild-type counterpart. Surprisingly, both **10d** and **14e** are potently cytotoxic to Jurkat J.γ1 cells with IC_{50} values of 1 and 2 μM, respectively. Comparatively, the IC_{50}'s of **10d** and **14e** against the healthy mammalian cell line Vero were estimated to be greater than 20 μM, the highest tested concentration (Table 3). To evaluate indirectly the contribution of HDAC6 inhibition to the anticancer activity of the compounds, the antiproliferative activity of HDAC6-selective inhibitor tubastatin A was evaluated against these cell lines. Although tubastatin A was as potent as **10d** and **14e** in Jurkat cells, it was 2- to 3-fold less potent against LNCaP and was inactive against Jurkat J.γ1 (Table 3). Given that the pan-inhibitor SAHA and HDAC6-selective tubastatin A are inactive against Jurkat J.γ1, the cytotoxic activity of lead compounds **10d** and **14e** against against Jurkat J.γ1 could be through inhibition of other yet to be identified cellular target(s).

Toward identifying other possible targets of the lead compounds **10d** and **14e**, we screened for their effect on the activity of a collection of matrix metalloproteases (MMPs) that have been suggested to play roles in apoptosis.[29] The rationale for screening against MMPs is based on the fact that 3HPT has been previously used as a ZBG in the design of MMP inhibitors.[30] At the tested concentration of 10 μM, **10d** and **14e** were inactive against MMP1, 2, 3, 7, 9, and 14, whereas the activity of MMP13 was halved at this very high concentration (Figure S4). Despite the marginal effect on MMP13, these proteins are not likely to be affected directly by the compounds tested.

We also tested lead compounds against HDAC2, which has been shown to be upregulated in certain malignancies and whose inhibition could result in apoptosis.[31,32] However, the IC_{50} values of **10d** and **14e** were 5840 ± 740 and 3680 ± 800 nM, respectively, suggesting that HDAC2 is not likely a direct target.

Intracellular Target Validation. The data presented showed that the lead 3HPT compounds possess HDAC6 inhibition activities (Table 2); nevertheless, we sought to confirm the involvement of HDAC6 inhibition in the mechanism of action of compounds **10d** and **14e**. Using western blotting, we examined the level of tubulin acetylation, a common marker for intracellular HDAC6 activity, in LNCaP cells following exposure to **10d** and **14e**.[33] We used SAHA as a positive control in this experiment. We observed that **10d** and **14e** increased tubulin acetylation but to a lesser extent than SAHA (Figure 4). These data propose that lead compounds **10d** and **14e** may derive their antiproliferative effects from an HDAC6-dependent pathway.

CONCLUSIONS

We have previously reported 3HPT as an advantageous ZBG for HDAC inhibition. Early SAR studies led to aryl- and diaryl-3HPT compounds that are devoid of HDAC1 inhibition activity but possess inhibitory activity against HDAC6 or HDAC8.[9] Herein, we have delineated the depth of the SAR of

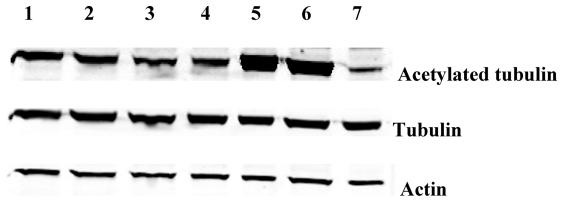

Figure 4. Western blot analysis of tubulin acetylation (HDAC6 inhibition) in the LNCaP cell line. Lane 1, **10d** (20 μM); lane 2, **10d** (5.43 μM); lane 3, **14e** (20 μM); lane 4, **14e** (3.49 μM); lane 5, **SAHA** (20 μM); lane 6, **SAHA** (2.31 μM); and lane 7, control.

dx.doi.org/10.1021/jm401225q | J. Med. Chem. 2013, 56, 9969−9981

3HPT-derived HDACi. The current efforts resulted in two lead compounds, **10d** and **14e**, demonstrating potent HDAC6 and HDAC8 activities without targeting HDAC1. Additionally, these new HDACi's enhanced tubulin acetylation in the LNCaP cell line and possessed antiproliferative activities against various cancer cell lines including Jurkat J.γ1 for which SAHA, tubastatin A, and the previously disclosed 3HPT-derived HDACi were inactive.

EXPERIMENTAL SECTION

Materials and Methods. Bromoalkanoic acid, benzyl bromide, 4-bromobenzylbromide, 4-(bromomethyl)-1,1′-biphenyl, 3-methoxy-2(1*H*)-pyridone, propargyl bromide, phenylacetylene, and representative boronic acids were purchased from either Sigma-Aldrich or Alfa Aesar. Alkynes **16** and **18**, which we could not obtain from commercial sources, were synthesized using the Bestmann−Ohira reagent as described previously (see the Supporting Information).[10,34,35] Anhydrous solvents and other reagents were purchased and used without further purification. Analtech silica gel plates (60 F_{254}) were used for analytical TLC, and Analtech preparative TLC plates (UV 254, 2000 μm) were used for purification. UV light was used to examine the spots. Silica gel (200−400 mesh) was used in column chromatography. NMR spectra were recorded on a Varian-Gemini 400 magnetic resonance spectrometer. ^{1}H NMR spectra were recorded in parts per million (ppm) relative to the peak of $CDCl_3$, (7.24 ppm), CD_3OD (3.31 ppm), or DMSO-d_6 (2.49 ppm). ^{13}C spectra were recorded relative to the central peak of the $CDCl_3$ triplet (77.0 ppm), CD_3OD (49.0 ppm), or the DMSO-d_6 septet (39.7 ppm) with complete heterodecoupling. Multiplicities are described using the abbreviations s, singlet; d, doublet, t, triplet; q, quartet; m, multiplet; and app, apparent. High-resolution mass spectra were recorded at the Georgia Institute of Technology mass spectrometry facility in Atlanta. All final 3HPT-based compounds were established to be >95% pure using HPLC. These HPLC analyses were done on a Beckman Coulter instrument with a Phenomenex RP C-18 column (250 mm × 4.6 mm) using a water (solvent A) and acetonitrile (solvent B) gradient starting from 40 to 80% of B over 20 min and constant at 80% for 5 min. The flow rate was 1 mL/min, and detection was at 379 nm. DU-145, LNCaP, and Jurkat J.λ1 were obtained from ATCC (Manassas, VA, USA). The Jurkat E6-1 cell line was kindly donated by Dr. John McDonald and grown in recommended medium supplemented with 10% fetal bovine serum (Global Cell Solutions, Charlottesville, VA, USA) and 1% pen/strep (Cellgro, Manassas, VA, USA) at 37 °C in an incubator with 5% CO_2. Mouse anti-acetylated α-tubulin antibody was obtained from Invitrogen (Life Technologies, Grand Island, NY, USA). Rabbit anti-actin and rabbit anti-tubulin α antibodies and tubastatin A were purchased from Sigma-Aldrich (St. Louis, MO, USA). Secondary antibodies (goat anti-rabbit conjugated to IRDye680 and goat anti-mouse conjugated to IRDye800) were purchased from LI-COR Biosciences (Lincoln, NE, USA). The CellTiter 96 aqueous one solution cell proliferation assay (MTS) kit was purchased from Promega (Madison, WI, USA).

Histone Deacetylase Inhibition. The HDAC activity in the presence of various compounds was assessed by SAMDI mass spectrometry. As a label-free technique, SAMDI is compatible with a broad range of native peptide substrates without requiring potentially disruptive fluorophores. To obtain IC_{50} values, we incubated isoform-optimized substrates (50 μM, detailed below) with enzyme (250nM, detailed below) and inhibitor (at concentrations ranging from 10 nM to 1.0 mM) in HDAC buffer (25.0 mM Tris-HCl, pH 8.0, 140 mM NaCl, 3.0 mM KCl, 1.0 mM $MgCl_2$, and 0.1 mg/mL BSA) in 96-well microtiter plates (60 min, 37 °C). Solution-phase deacetylation reactions were quenched with trichostatin A (TSA) and transferred to SAMDI plates to immobilize the substrate components. SAMDI plates were composed of an array of self-assembled monolayers (SAMs) presenting maleimide in standard 384-well format for high-throughput handling capability. Following immobilization, plates were washed to remove buffer constituents, enzyme, inhibitor, and any unbound substrate and analyzed by MALDI mass spectrometry using automated protocols.[17] Deacetylation yields in each triplicate sample were determined from the integrated peak intensities of the molecular ions for the substrate and the deacetylated product ion by taking the ratio of the former over the sum of both. Yields were plotted with respect to inhibitor concentration and fitted to obtain IC_{50} values for each isoform−inhibitor pair.

Isoform-optimized substrates were prepared by traditional FMOC solid-phase peptide synthesis (reagents supplied by Anaspec) and purified by semi-preparative HPLC on a reverse-phase C18 column (Waters). The peptide GRK^{ac}FGC was prepared for HDAC1 and HDAC8 experiments, whereas the peptide GRK^{ac}YGC was prepared for HDAC6 and HDAC2 experiments. Isoform preference for the indicated substrates was determined by earlier studies on peptide arrays.[36]

HDAC1, HDAC6, and HDAC2 were purchased from BPS Biosciences. The catalytic domain of HDAC8 was expressed as previously reported.[36] Briefly, an amplicon was prepared by PCR with the following primers: forward (5′−3′) TATTCTCGAGGA-CCACATGCTTCA and reverse (5′−3′) ATAAGCTAGCATG-GAGGAGCCGGA. A pET21a construct bearing the genetic insert between the NheI and XhoI restriction sites was transformed into *Escherichia coli* BL21(DE3) (Lucigen) and expressed by standard protocols. Following purification by affinity chromatography, the His-tagged enzyme-containing fractions were purified by FPLC (AKTA) on a superdex size-exclusion column (GE), spin-concentrated, and stored at −80 °C in HDAC buffer with 10% glycerol.

Molecular Docking analysis. The docking studies were performed as previously reported with Autodock Vina through PyRx.[37,38] Following the 3D energy minimization of the ligand by ChemBioDraw 3D, the docking was run in a 25 Å cubic space encompassing the active site, the binding pocket, and its surrounding.

Cell Viability Assay. DU-145 and Vero cells were maintained in EMEM and DMEM, respectively, supplemented with 10% FBS and 1% pen/strep, and all other cell lines were maintained in RPMI 1640 supplemented with 10% FBS and 1% pen/strep. DU-145, Vero, and LNCaP cells were incubated on a 96-wells plate for 24 h prior to a 72 h drug treatment, whereas Jurkat and Jurkat J.γ1 cells were incubated in media containing the various compounds for 72 h. Cell viability was measured using the MTS assay according to the manufacturer's protocol. The DMSO concentration in the cell media during the cell viability experiment was maintained at 0.1%.

Western Blot Analysis for Tubulin Acetylation. LNCaP cells were plated for 24 h and treated with various concentrations of compounds for 4 h. The cells were washed with PBS buffer and resuspended in CelLyticM buffer containing a cocktail of protease inhibitors (Sigma-Aldrich, St. Louis, MO, USA). Following quantification through a Bradford protein assay, equal amounts of protein were loaded onto an SDS-page gel (Bio-Rad, Hercules, CA, USA) and resolved by electrophoresis at a constant voltage of 100 V for 2 h. The gel was transferred onto a nitrocellulose membrane and probed for acetylated tubulin and tubulin as well as actin as a loading control.

MMP Assay. MMP inhibitor profiling kit was purchased from Enzo Life Sciences (Farmingdale, NY, USA). The selection of MMPs tested was guided by the reported antiproliferative activity of AG3340, an MMP inhibitor selective for isoforms 1, 2, 3, 7, 9, 13, and 14.[29] Each MMP was incubated with the inhibitor (10 μM) for 30 min at 37 °C in the assay buffer. The OmniMMP fluorogenic substrate peptide was added, and the reaction was allowed to proceed at 37 °C for 30 min. The fluorescence was measured using a fluorescence plate reader with excitation at 328 nm and emission at 420 nm.[39]

Statistical Analysis. The values are reported as the mean ± SD from at least two independent experiments performed in triplicate. The Student's *t* test was performed in Excel, and results with *p* value less than 5% were considered statistically different.

Representative Procedure for the Conversion of Azidoalkanol to Azidoalkyl Methanesulfonate 5. Synthesis of 2-Azidoethyl Methanesulfonate (5a). To a solution of compound 2-azidoethanol (1.00 g, 11.49 mmol) in THF (25 mL) and triethylamine (Et_3N) (2.418 mL, 17.24 mmol) was added mesyl chloride (1.328 mL, 17.24 mmol) at 0 °C, and the mixture was allowed

to warm to room temperature. Stirring continued for 3 h, during which TLC revealed a quantitative conversion into a higher R_f product. CH_2Cl_2 (70 mL) and saturated sodium bicarbonate (50 mL) were added, and the two layers were separated. The organic layer was washed with sodium bicarbonate (2 × 50 mL) and saturated brine (45 mL) and dried over Na_2SO_4. Solvent was evaporated off to give crude compound **5a** (1.70 g) as a colorless oil, which was used for next step without further purification. A similar procedure was used for the synthesis of **5b–f**.

Representative Procedure for the Synthesis of 1-(2-Azidoalkyl)-3-methoxypyridin-2-ones. Synthesis of 6-1-(2-Azidoethyl)-3-methoxypyridin-2-one (6a). A mixture of 3-methoxypyridin-2-one (0.40 g, 3.20 mmol), **5a** (0.79 g, 4.80 mmol), and K_2CO_3 (1.32 g, 9.60 mmol) in THF was stirred under refluxing conditions overnight. The reaction mixture was cooled to room temperature and partitioned between CH_2Cl_2 (60 mL) and water (50 mL), and the two layers were separated. The organic layer was washed with water (2 × 35 mL) and brine (1 × 30 mL), dried on Na_2SO_4, and evaporated in vacuo. The crude product was purified by flash chromatography, eluting with a step gradient of acetone in CH_2Cl_2 (max 15%) to give 0.34 g of **6a** (55%) as a colorless oil. ^{1}H NMR (400 MHz, $CDCl_3$) δ 6.77 (dd, J = 6.9, 1.6 Hz, 1H), 6.48 (dd, J = 7.5, 1.6 Hz, 1H), 5.96 (m, 1H), 3.91 (m, 2H), 3.62 (s, 3H), 3.52 (m, 2H). ^{13}C NMR (100 MHz, $CDCl_3$) δ 157.39, 149.41, 128.61, 112.16, 104.37, 55.36, 49.00, 48.91. HRMS (EI) calcd for $C_8H_{10}N4O_2$ $[M]^+$, 194.0804; found, 194.0816.

*1-(3-Azidopropyl)-3-benzyloxypyridin-2-one (**6b**).* Reaction of 3-benzyloxypyridin-2-one (0.40 g, 1.99 mmol) and **5b** (0.53 g, 2.98 mmol) within 16 h as described for the synthesis of **6a** gave compound **6b** (0.30 g, 53%) as a colorless oil. ^{1}H NMR (300 MHz, $CDCl_3$) δ 7.28 (m, 5H), 6.84 (dd, J = 6.9, 1.6 Hz, 1H), 6.60 (dd, J = 7.4, 1.5 Hz, 1H), 5.98 (t, J = 7.1 Hz, 1H), 4.96 (s, 2H), 3.97 (t, J = 6.8 Hz, 2H), 3.28 (t, J = 6.5 Hz, 2H), 1.98 (p, J = 6.7 Hz, 2H). ^{13}C NMR (75 MHz, $CDCl_3$) δ 157.78, 148.65, 135.93, 128.85, 128.24, 127.69, 127.03, 115.16, 104.53, 70.39, 48.14, 47.06, 27.66. HRMS (EI) calcd for $C_{15}H_{16}N_4O_2$ $[M]^+$, 284.1273; found, 284.1271.

*1-(4-Azidobutyl)-3-benzyloxypyridin-2-one (**6c**).* Reaction of 3-benzyloxypyridin-2-one (0.40 g, 1.99 mmol) and **5c** (0.58 g, 2.98 mmol) within 16 h as described for the synthesis of **6a** gave compound **6c** (0.36 g, 62%) as a colorless oil. ^{1}H NMR (400 MHz, $CDCl_3$) δ 7.22 (m, 5H), 6.78 (dd, J = 6.9, 1.7 Hz, 1H), 6.54 (dd, J = 7.4, 1.7 Hz, 1H), 5.91 (m, 1H), 4.96 (s, 2H), 3.85 (t, J = 7.2 Hz, 2H), 3.17 (t, J = 6.8 Hz, 2H), 1.71 (m, 2H), 1.48 (m, 2H). ^{13}C NMR (100 MHz, $CDCl_3$) δ 157.52, 148.27, 135.78, 128.37, 127.98, 127.42, 126.82, 114.92, 104.32, 70.09, 50.43, 48.46, 25.83, 25.42. HRMS (EI) calcd for $C_{16}H_{18}N_4O_2$ $[M]^+$, 298.1430; found, 298.1446.

*1-(5-Azidopentyl)-3-benzyloxypyridin-2-one (**6d**).* Reaction of 3-benzyloxypyridin-2-one (0.50 g, 2.49 mmol) and **5d** (0.62 g, 2.98 mmol) within 16 h as described for the synthesis of **6a** gave compound **6d** (0.49 g, 63%) as a colorless oil. ^{1}H NMR (400 MHz, $CDCl_3$) δ 7.35 (d, J = 8.0 Hz, 2H), 7.23 (m, 3H), 6.81 (m, 1H), 6.56 (m, 1H), 5.94 (m, 1H), 5.01 (s, 2H), 3.85 (m, 2H), 3.18 (m, 2H), 1.71 (m, 2H), 1.54 (m, 2H), 1.32 (m, 2H). ^{13}C NMR (100 MHz, $CDCl_3$) δ 157.68, 148.47, 135.98, 128.60, 128.12, 127.53, 126.93, 115.09, 104.32, 70.27, 50.77, 49.21, 28.19, 28.06, 23.37. HRMS (EI) calcd for $C_{17}H_{20}N_4O_2$ $[M]^+$, 312.1586; found, 312.1589.

*1-(6-Azidohexyl)-3-benzyloxypyridin-2-one (**6e**).* Reaction of 3-benzyloxypyridin-2-one (0.50 g, 2.49 mmol) and **5e** (0.66 g, 2.98 mmol) within 16 h as described for the synthesis of **6a** gave compound **6e** (0.48 g, 60%) as a colorless oil. ^{1}H NMR (400 MHz, $CDCl_3$) δ 7.15 (m, 5H), 6.65 (dd, J = 7.4, 1.8 Hz, 1H), 6.45 (dd, J = 7.4, 1.8 Hz, 1H), 5.81 (t, J = 7.1 Hz, 1H), 4.92 (s, 2H), 3.76 (t, J = 6.8 Hz, 2H), 3.05 (t, J = 6.8 Hz, 2H), 1.58 (m, 2H), 1.40 (m, 2H), 1.90 (m, 4H). ^{13}C NMR (100 MHz, $CDCl_3$) δ 157.55, 148.25, 135.95, 128.60, 128.10, 126.95, 126.50, 115.05, 104.90, 70.50, 51.05, 49.20, 28.65, 28.50, 26.20, 25.80. HRMS (FAB) calcd for $C_{18}H_{23}N_4O_2$ $[M + H]^+$, 327.1821; found, 327.1848.

*1-(7-Azidoheptyl)-3-benzyloxypyridin-2-one (**6f**).* Reaction of 3-benzyloxypyridin-2-one (0.79 g, 3.38 mmol) and **5f** (0.81 g, 4.05 mmol) within 16 h as described for the synthesis of **6a** gave compound **6f** (0.55 g, 48%) as a colorless oil. ^{1}H NMR (400 MHz, $CDCl_3$) δ 7.42 (dd, J = 7.8, 1.0 Hz, 2H), 7.31 (m, 3H), 6.85 (dd, J = 6.9, 1.7 Hz, 1H), 6.61 (dd, J = 7.4, 1.7 Hz, 1H), 5.99 (m, 1H), 5.09 (s, 2H), 3.93 (m, 2H), 3.23 (t, J = 6.9 Hz, 2H), 1.74 (m, 2H), 1.55 (m, 2H), 1.34 (m, 6H). ^{13}C NMR (100 MHz, $CDCl_3$) δ 158.32, 149.19, 136.63, 129.15, 128.74, 128.13, 127.52, 115.66, 104.69, 94.66, 70.96, 51.62, 50.03, 29.22, 28.98, 26.77, 26.72.

Representative Procedure for Synthesis of 7. Synthesis of 1-Phenyltriazolylethyl-3-methoxypyridin-2-one (7a). Phenylacetylene (0.17 g, 1.67 mmol) and **6a** (0.27 g, 1.36 mmol) were dissolved in anhydrous THF (10 mL) and stirred under argon at room temperature. Copper(I) iodide (0.01 g, 0.07 mmol) and Hunig's base (0.1 mL) were added to the reaction mixture, and stirring was continued for 4 h. The reaction mixture was diluted with CH_2Cl_2 (40 mL) and washed with 1:4 NH_4OH/saturated NH_4Cl (3 × 30 mL) and saturated NH_4Cl (30 mL). The organic layer was dried over Na_2SO_4 and concentrated in vacuo. The crude product was triturated with hexanes to give 366 mg (91%) of white solid **7a**. ^{1}H NMR (400 MHz, $CDCl_3$) δ 7.68 (s, 1H), 7.47 (d, J = 7.5 Hz, 2H), 7.11 (m, 3H), 6.43 (d, J = 7.4 Hz, 1H), 6.35 (dd, J = 6.8, 0.9 Hz, 1H), 5.78 (t, J = 7.2 Hz, 1H), 4.57 (t, J = 5.7 Hz, 2H), 4.25 (t, J = 5.6 Hz, 2H), 3.53 (s, 3H). ^{13}C NMR (100 MHz, $CDCl_3$) δ 157.70, 149.08, 147.21, 129.40, 128.30, 128.08, 127.80, 125.00, 120.91, 113.02, 105.44, 55.15, 49.72, 47.44. HRMS (EI) calcd for $C_{16}H_{16}N_4O_2$ $[M]^+$, 296.1273; found, 296.1268.

*1-Phenyltriazolylpropyl-3-benzyloxypyridin-2-one (**7b**).* Reaction of phenylacetylene (0.13 g, 1.25 mmol) and **6b** (0.30 g, 1.04 mmol) within 4 h as described for the synthesis of **7a** gave compound **7b** (0.31 g, 77%) as a white solid. ^{1}H NMR (400 MHz, $CDCl_3$) δ 8.00 (s, 1H), 7.77 (d, J = 7.3 Hz, 2H), 7.27 (m, 8H), 6.88 (d, J = 5.7 Hz, 1H), 6.57 (d, J = 6.4 Hz, 1H), 5.95 (t, J = 7.1 Hz, 1H), 4.99 (s, 2H), 4.34 (t, J = 6.4 Hz, 2H), 3.94 (t, J = 6.4 Hz, 2H), 2.32 (m, 2H). ^{13}C NMR (100 MHz, $CDCl_3$) δ 157.92, 148.47, 147.30, 135.73, 130.26, 128.81, 128.49, 128.22, 127.76, 127.71, 127.01, 125.33, 120.16, 114.95, 104.83, 70.33, 47.00, 46.48, 29.30. HRMS (EI) calcd for $C_{23}H_{22}N_4O_2$ $[M]^+$, 386.1743; found, 386.1734.

*1-Phenyltriazolylbutyl-3-benzyloxypyridin-2-one (**7c**).* Reaction of phenylacetylene (0.12 g, 1.18 mmol) and **6c** (0.30 g, 1.01 mmol) within 4 h as described for the synthesis of **7a** gave compound **7c** (0.31 g, 77%) as a white solid. ^{1}H NMR (400 MHz, $CDCl_3$) δ 7.83 (s, 1H), 7.76 (m, 2H), 7.26 (m, 8H), 6.76 (dd, J = 6.9, 1.5 Hz, 1H), 6.56 (dd, J = 7.4, 1.5 Hz, 1H), 5.91 (t, J = 7.1 Hz, 1H), 4.99 (s, 2H), 4.31 (m, 2H), 3.89 (t, J = 7.1 Hz, 2H), 1.85 (m, 2H), 1.67 (m, 2H). ^{13}C NMR (100 MHz, $CDCl_3$) δ 157.71, 148.38, 147.20, 135.83, 130.29, 128.45, 128.41, 128.16, 127.68, 127.63, 126.96, 125.25, 119.87, 114.99, 104.60, 70.26, 49.11, 48.02, 26.78, 25.65. HRMS (EI) calcd for $C_{24}H_{24}N_4O_2$ $[M]^+$, 400.1899; found, 400.1888.

*1-Phenyltriazolylpentyl-3-benzyloxypyridin-2-one (**7d**).* Reaction of phenylacetylene (0.04 g, 0.39 mmol) and **6d** (0.10 g, 0.32 mmol) within 4 h as described for the synthesis of **7a** gave compound **7d** (0.09 g, 72%) as a white solid. ^{1}H NMR (400 MHz, $CDCl_3$) δ 7.78 (m, 3H), 7.30 (m, 8H), 6.79 (d, J = 6.8 Hz, 1H), 6.57 (d, J = 7.3 Hz, 1H), 5.94 (t, J = 7.1 Hz, 1H), 5.02 (s, 2H), 4.31 (t, J = 7.0 Hz, 2H), 3.87 (t, J = 7.2 Hz, 2H), 1.91 (m, 2H), 1.74 (m, 2H), 1.30 (m, 2H). ^{13}C NMR (100 MHz, $CDCl_3$) δ 157.80, 148.57, 147.39, 136.02, 130.44, 128.64, 128.56, 128.27, 127.81, 127.71, 127.05, 125.40, 119.57, 115.12, 104.49, 70.40, 49.71, 49.06, 29.42, 28.03, 23.05.

*1-Phenyltriazolylhexyl-3-benzyloxypyridin-2-one (**7e**).* Reaction of phenylacetylene (0.08 g, 0.78 mmol) and **6e** (0.21 g, 0.65 mmol) within 4 h as described for the synthesis of **7a** gave compound **7e** (0.16 g, 58%) as a white solid. NMR (400 MHz, $CDCl_3$) δ 7.66 (m, 3H), 7.20 (m, 8H), 6.68 (dd, J = 6.9, 1.5 Hz, 1H), 6.46 (dd, J = 7.4, 1.5 Hz, 1H), 5.82 (t, J = 7.1 Hz, 1H), 4.92 (s, 2H), 4.18 (t, J = 6.8 Hz, 2H), 3.75 (t, J = 6.8 Hz, 2H), 1.76 (m, 2H), 1.56 (m, 2H), 1.19 (m, 4H). ^{13}C NMR (100 MHz, $CDCl_3$) δ 157.64, 148.46, 147.27, 135.95, 130.36, 128.57, 128.48, 128.19, 127.72, 127.60, 126.96, 125.32, 119.37, 115.02, 104.37 70.45, 50.03, 49.35, 29.90, 28.66, 25.87, 25.78. HRMS (FAB) calcd for $C_{26}H_{29}N_4O_2$ $[M + H]^+$, 429.2290; found, 429.2291.

*1-Phenyltriazolylheptyl-3-benzyloxypyridin-2-one (**7f**).* Reaction of phenylacetylene (0.09 g, 0.88 mmol) and **6f** (0.25 g, 0.74 mmol)

within 4 h as described for the synthesis of **7a** gave compound **7f** (0.23 g, 70%) as a white solid. ^{1}H NMR (400 MHz, $CDCl_3$) δ 7.79 (m, 3H), 7.31 (m, 8H), 6.83 (dd, J = 6.9, 1.7 Hz, 1H), 6.60 (dd, J = 7.4, 1.7 Hz, 1H), 5.97 (t, J = 7.1 Hz, 1H), 5.07 (s, 2H), 4.35 (t, J = 7.1 Hz, 2H), 3.91 (m, 2H), 1.88 (m, 2H), 1.71 (m, 2H), 1.32 (d, J = 10.0 Hz, 6H). ^{13}C NMR (100 MHz, $CDCl_3$) δ 158.31, 149.13, 147.92, 136.57, 130.93, 129.15, 129.04, 128.74, 128.28, 128.15, 127.51, 125.90, 125.86, 119.75, 115.60, 104.79, 70.92, 50.52, 49.90, 30.42, 29.13, 28.72, 26.53, 26.46. HRMS (FAB) calcd for $C_{27}H_{31}N_4O_2$ $[M + H]^+$, 443.2447; found, 443.2494.

*1-Phenyltriazolylethyl-3-hydroxypyridin-2-one (**8a**).* To a solution of **7a** (0.10 g, 0.34 mmol) in dry CH_2Cl_2 (8 mL) was slowly added 1 M BBr_3 (1.2 equiv) at −30 °C under an argon atmosphere. The reaction mixture was stirred for 48 h at room temperature. The mixture was again cooled to −30 °C, and MeOH (5 mL) was slowly added to the mixture. After evaporation of the solvent, the residue was adjusted to pH 7 with 1 M NaOH and then extracted with $CHCl_3$ (30 mL × 3). The combined organic layers were dried over Na_2SO_4 to give 0.08 g (83%) of **8a** as slightly brownish solid without any further purification required. ^{1}H NMR (400 MHz, DMSO) δ 9.11 (s, 1H), 8.51 (s, 1H), 7.78 (d, J = 7.3 Hz, 2H), 7.43 (t, J = 7.6 Hz, 2H), 7.31 (t, J = 7.3 Hz, 1H), 6.75 (d, J = 5.9 Hz, 1H), 6.64 (d, J = 6.0 Hz, 1H), 5.95 (t, J = 7.0 Hz, 1H), 4.76 (t, J = 5.5 Hz, 2H), 4.42 (t, J = 5.6 Hz, 2H). ^{13}C NMR (100 MHz, DMSO) δ 158.25, 147.17, 146.77, 131.11, 129.34, 128.41, 128.31, 125.54, 122.23, 115.38, 105.76, 49.42, 48.33. HRMS (EI) calcd for $C_{15}H_{14}N_4O_2$ $[M]^+$, 282.1117; found, 282.1120.

*1-Phenyltriazolylpropyl-3-hydroxypyridin-2-one (**8b**).* To a solution of **7b** (0.29 g, 0.75 mmol) in CH_2Cl_2/EtOAc/MeOH (2:2:1, 10 mL) was added 10% Pd on carbon (15 mg). The reaction was stirred under ballon hydrogen pressure for 5 h. The reaction mixture was filtered, and the solvent was evaporated. Column chromatography eluting with a step gradient of acetone in CH_2Cl_2 (max 20%) gave pure **8b** (0.19 g, 85%) as a slightly brownish solid. ^{1}H NMR (400 MHz, DMSO) δ 9.03 (s, 1H), 8.62 (s, 1H), 7.82 (d, J = 7.6 Hz, 2H), 7.38 (m, 3H), 7.15 (d, J = 6.6 Hz, 1H), 6.68 (d, J = 6.4 Hz, 1H), 6.11 (t, J = 6.7 Hz, 1H), 4.43 (t, J = 6.4 Hz, 2H), 3.99 (m, 2H), 2.27 (m, 2H). ^{13}C NMR (100 MHz, $CDCl_3$) δ 147.49, 129.71, 128.52, 127.99, 125.29, 120.42, 107.98, 66.61, 47.10, 29.27. HRMS (EI) calcd for $C_{16}H_{16}N_4O_2$ $[M]^+$, 296.1273; found, 296.1274.

*1-Phenyltriazolylbutyl-3-hydroxypyridin-2-one (**8c**).* Reaction of **7c** (0.25 g, 0.62 mmol) in anhydrous THF as described for the synthesis of **8b** gave **8c** (0.12 g, 63%). ^{1}H NMR (400 MHz, $CDCl_3$) δ 7.79 (m, 3H), 7.41 (t, J = 7.6 Hz, 2H), 7.32 (t, J = 7.4 Hz, 1H), 6.76 (m, 3H), 6.13 (t, J = 7.2 Hz, 1H), 4.45 (t, J = 6.8 Hz, 2H), 4.02 (t, J = 7.1 Hz, 2H), 1.99 (m, 2H), 1.82 (m, 2H). ^{13}C NMR (100 MHz, $CDCl_3$) δ 158.47, 147.63, 146.62, 130.41, 128.69, 127.99, 126.60, 125.53, 119.80, 114.15, 107.10, 49.38, 48.57, 27.02, 26.01. HRMS (EI) calcd for $C_{17}H_{18}N_4O_2$ $[M]^+$, 310.1430; found, 310.1425.

*1-Phenyltriazolylpentyl-3-hydroxypyridin-2-one (**8d**).* Reaction of **7d** (0.09 g, 0.20 mmol) in anhydrous THF as described for the synthesis of **8b** gave **8d** (0.05 g, 77%). ^{1}H NMR (400 MHz, DMSO) δ 8.56 (s, 1H), 7.82 (d, J = 8.1 Hz, 2H), 7.43 (t, J = 7.7 Hz, 2H), 7.32 (t, J = 7.4 Hz, 1H), 7.10 (dd, J = 6.8, 1.6 Hz, 1H), 6.65 (dd, J = 7.2, 1.5 Hz, 1H), 6.05 (t, J = 7.0 Hz, 1H), 4.38 (t, J = 7.0 Hz, 2H), 3.89 (t, J = 7.2 Hz, 2H), 1.89 (m, 2H), 1.67 (m, 2H), 1.25 (m, 2H). ^{13}C NMR (100 MHz, $CDCl_3$) δ 158.44, 147.67, 146.61, 130.51, 128.72, 128.01, 126.71, 125.57, 119.54, 113.81, 106.86, 49.86, 49.38, 29.58, 28.31, 23.19. HRMS (FAB) calcd for $C_{18}H_{21}N_4O_2$ $[M + H]^+$, 325.1664; found, 325.1683.

*1-Phenyltriazolylhexyl-3-hydroxypyridin-2-one (**8e**).* Reaction of **7e** (0.15 g, 0.35 mmol) in anhydrous THF as described for the synthesis of **8b** gave **8e** (0.081 g, 69%). ^{1}H NMR (400 MHz, $CDCl_3$) δ 7.81 (m, 3H), 7.42 (m, 2H), 7.32 (m, 1H), 6.77 (m, 2H), 6.12 (t, J = 7.1 Hz, 1H), 4.38 (t, J = 7.1 Hz, 2H), 3.95 (m, 2H), 1.95 (m, 2H), 1.76 (d, J = 7.0 Hz, 2H), 1.39 (m, 4H). ^{13}C NMR (100 MHz, $CDCl_3$) δ 158.20, 147.25, 146.40, 130.30, 128.60, 127.85, 126.65, 125.40, 119.65, 113.90, 106.80, 50.20, 49.60, 30.05, 28.95, 26.00, 25.90. HRMS (FAB) calcd for $C_{19}H_{23}N_4O_2$ $[M + H]^+$, 339.1821; found, 339.1814.

*1-Phenyltriazolylheptyl-3-hydroxypyridin-2-one (**8f**).* Reaction of **7f** (0.22 g, 0.50 mmol) in anhydrous THF as described for the synthesis of **8b** gave **8f** (0.13 g, 74%). ^{1}H NMR (400 MHz, DMSO) δ 8.91 (s, 1H), 8.57 (s, 1H), 7.82 (d, J = 7.4 Hz, 2H), 7.42 (t, J = 7.6 Hz, 2H), 7.31 (t, J = 7.3 Hz, 1H), 7.09 (d, J = 6.6 Hz, 1H), 6.64 (d, J = 7.0 Hz, 1H), 6.04 (t, J = 6.9 Hz, 1H), 4.36 (t, J = 7.0 Hz, 2H), 3.86 (t, J = 7.2 Hz, 2H), 1.83 (m, 2H), 1.61 (m, 2H), 1.26 (m, 6H). ^{13}C NMR (100 MHz, $CDCl_3$) δ 158.80, 147.89, 147.00, 130.88, 129.05, 128.30, 127.12, 125.87, 119.83, 114.13, 107.10, 50.48, 50.05, 30.37, 29.20, 28.67, 26.46, 26.42. HRMS (FAB) calcd for $C_{20}H_{25}N_4O_2$ $[M + H]^+$, 353.1977; found, 353.1992.

*1-Phenyltriazolylethyl-3-methoxypyridine-2-thione (**9**).* To a stirring solution of Lawesson's reagent (0.08 g, 0.19 mmol) in toluene (10 mL) was added starting material **7a** (0.10g, 0.33 mmol), and the reaction mixture was heated at refluxing temperature overnight. The reaction mixture was cooled to room temperature, and the solvent was evaporated under reduced pressure. The crude product was purified by preparative TLC, eluting with $CHCl_3$/acetone/EtOH (10:1:0.2) to give **9** (0.07 g, 68%) as a yellow solid. ^{1}H NMR (400 MHz, $CDCl_3$) δ 7.69 (d, J = 7.4 Hz, 2H), 7.56 (s, 1H), 7.35 (t, J = 7.5 Hz, 2H), 7.28 (m, 1H), 6.97 (d, J = 6.6 Hz, 1H), 6.62 (d, J = 7.8 Hz, 1H), 6.37 (m, 1H), 5.13 (t, J = 5.6 Hz, 2H), 5.03 (t, J = 5.6 Hz, 2H), 3.86 (s, 3H). ^{13}C NMR (100 MHz, $CDCl_3$) δ 171.92, 158.94, 147.52, 132.68, 129.92, 128.69, 128.14, 125.43, 120.96, 111.72, 110.22, 56.72, 56.63, 46.38. HRMS (EI) calcd for $C_{16}H_{16}N_4OS$ $[M]^+$, 312.1045; found, 312.1039.

*1-Phenyltriazolylethyl-3-hydroxypyridine-2-thione (**10a**).* To a solution of **9** (0.06 g, 0.19 mmol) in dry CH_2Cl_2 (8 mL) at −30 °C was slowly added 1 M BBr_3 in CH_2Cl_2 (0.22 mmol) under an argon atmosphere, and the reaction mixture was subsequently stirred for 48 h at room temperature. The mixture was cooled to −30 °C, and MeOH (5 mL) was slowly added. The solvent was evaporated off, and the residue was adjusted to pH 7 with aqueous 1 M NaOH and then extracted with $CHCl_3$ (3 × 30 mL). The combined organic layers were dried over Na_2SO_4, and the solvent was evaporated in vacuo to yield compound **10a** (0.06 g, 93%) as a dark violet solid. t_R 8.1 min. ^{1}H NMR (400 MHz, $CDCl_3$) δ 8.40 (s, 1H), 7.73 (d, J = 7.3 Hz, 2H), 7.51 (s, 1H), 7.40 (t, J = 7.5 Hz, 2H), 7.33 (t, J = 7.3 Hz, 1H), 6.95 (dd, J = 9.2, 7.2 Hz, 2H), 6.46 (m, 1H), 5.08 (m, 4H). ^{13}C NMR (100 MHz, $CDCl_3$) δ 168.47, 155.10, 147.75, 132.00, 129.82, 128.77, 128.30, 125.53, 120.90, 113.66, 112.61, 57.45, 46.41. HRMS (EI) calcd for $C_{15}H_{14}N_4OS$ $[M]^+$, 298.0888; found, 298.0888.

*1-Phenyltriazolylpropyl-3-hydroxypyridine-2-thione (**10b**).* Compound **8b** (0.06 g, 0.20 mmol) was ground together with P_4S_{10} (0.05g, 0.11 mmol) in a mortar and pestle to form a gray powder. The powder was stirred under argon in a flask fitted with a condenser and heated at 175 °C for 2 h. The reaction flask was covered with aluminum foil during the reaction. After 2 h of reaction, the flask was cooled to room temperature, 10% MeOH in CH_2Cl_2 (25 mL) was added, and stirring was continued for another 15 min. The reaction mixture then washed with water (2 × 30 mL), the organic layer was dried with Na_2SO_4, and the solvent was evaporated in vacuo. The crude product was purified by preparative TLC, eluting with 8% MeOH in CH_2Cl_2 to give **10b** (0.04 g, 64%) as an olive green solid. t_R 8.2 min. ^{1}H NMR (400 MHz, $CDCl_3$) δ 8.47 (s, 1H), 7.82 (m, 3H), 7.50 (d, J = 6.5 Hz, 1H), 7.43 (t, J = 7.5 Hz, 2H), 7.34 (t, J = 7.4 Hz, 1H), 6.97 (m, 1H), 6.66 (m, 1H), 4.62 (t, J = 6.9 Hz, 2H), 4.48 (m, 2H), 2.65 (m, 2H). ^{13}C NMR (100 MHz, $CDCl_3$) δ 168.59, 155.22, 148.03, 131.85, 130.17, 128.84, 128.29, 125.61, 119.84, 113.87, 112.28, 54.99, 46.95, 28.02. HRMS (EI) calcd for $C_{16}H_{16}N_4OS$ $[M]^+$, 312.1045; found, 312.1060.

*1-Phenyltriazolylbutyl-3-hydroxypyridine-2-thione (**10c**).* Reaction of **8c** (0.06 g, 0.18 mmol) and P_4S_{10} (0.05 g, 0.11 mmol) under neat conditions as described for the synthesis of **10b** gave compound **10c** (0.03 g, 51%) as an olive green solid. t_R 8.7 min. ^{1}H NMR (400 MHz, $CDCl_3$) δ 8.50 (s, 1H), 7.81 (m, 3H), 7.36 (m, 4H), 6.94 (d, J = 7.6 Hz, 1H), 6.62 (t, J = 6.8 Hz, 1H), 4.54 (t, J = 7.6 Hz, 2H), 4.46 (t, J = 6.4 Hz, 2H), 2.03 (m, 4H). ^{13}C NMR (100 MHz, $CDCl_3$) δ 168.51, 155.08, 147.73, 131.02, 130.36, 128.79, 128.13, 125.58, 119.91, 113.87, 112.10, 56.96, 49.41, 27.02, 25.08. HRMS (EI) calcd for $C_{17}H_{18}N_4OS$ $[M]^+$, 326.1201; found, 326.1200.

*1-Phenyltriazolylpentyl-3-hydroxypyridine-2-thione (**10d**).* Reaction of **8d** (0.03 g, 0.08 mmol) and P_4S_{10} (0.02 g, 0.05 mmol) under

dx.doi.org/10.1021/jm401225q | J. Med. Chem. 2013, 56, 9969−9981

neat conditions as described for the synthesis of **10b** gave compound **10d** (0.02 g, 73%) as an olive green solid. t_R 9.6 min. ^{1}H NMR (400 MHz, DMSO) δ 8.55 (d, J = 2.9 Hz, 2H), 7.83 (t, J = 7.8 Hz, 3H), 7.43 (q, J = 7.4 Hz, 2H), 7.32 (t, J = 6.6 Hz, 1H), 7.08 (m, 1H), 6.92 (dd, J = 31.0, 6.8 Hz, 1H), 6.81 (m, 1H), 4.51 (m, 2H), 4.41 (t, J = 7.0 Hz, 2H), 1.89 (m, 4H), 1.32 (m, 2H). ^{13}C NMR (100 MHz, $CDCl_3$) δ 168.37, 155.10, 147.66, 131.04, 130.46, 128.75, 128.05, 125.57, 119.68, 113.69, 111.96, 57.73, 49.73, 29.47, 27.12, 23.04. HRMS (EI) calcd for $C_{18}H_{20}N_4OS$ $[M]^+$, 340.1358; found, 340.1364.

*1-Phenyltriazolylhexyl-3-hydroxypyridine-2-thione (**10e**).* Reaction of **8e** (0.18 g, 0.53 mmol) and P_4S_{10} (0.12 g, 0.27 mmol) under neat conditions as described for the synthesis of **10b** gave compound **10e** (0.08 g, 43%) as an olive green semisolid. t_R 10.8 min. ^{1}H NMR (400 MHz, $CDCl_3$) δ 8.57 (s, 1H), 7.83 (d, J = 7.5 Hz, 2H), 7.76 (s, 1H), 7.41 (t, J = 7.5 Hz, 2H), 7.32 (m, 2H), 6.94 (m, 1H), 6.72 (m, 1H), 4.49 (m, 2H), 4.40 (t, J = 6.9 Hz, 2H), 1.97 (m, 4H), 1.36 (m, 4H). ^{13}C NMR (100 MHz, $CDCl_3$) δ 164.38, 162.90, 147.70, 130.54, 128.76, 128.03, 126.64, 125.61, 119.51, 118.75, 118.29, 59.74, 50.10, 29.91, 27.99, 25.82, 25.65. HRMS (ESI) calcd for $C_{19}H_{23}N_4OS$ $[M + H]^+$, 355.1587; found, 355.1632.

*1-Phenyltriazolylheptyl-3-hydroxypyridine-2-thione (**10f**).* Reaction of **8f** (0.12 g, 0.35 mmol) and P_4S_{10} (0.08 g, 0.17 mmol) under neat conditions as described for the synthesis of **10b** gave compound **10f** (0.05 g, 43%) as an olive green semisolid. t_R 12.1 min. ^{1}H NMR (400 MHz, DMSO) δ 8.55 (m, 1H), 7.81 (d, J = 8.2 Hz, 2H), 7.65 (d, J = 6.2 Hz, 1H), 7.42 (m, 2H), 7.30 (m, 1H), 7.02 (m, 1H), 6.85 (m, 1H), 4.50 (m, 2H), 4.36 (t, J = 7.1 Hz, 2H), 1.85 (d, J = 7.0 Hz, 4H), 1.33 (s, 6H). ^{13}C NMR (100 MHz, $CDCl_3$) δ 147.76, 130.66, 128.76, 130.39, 128.98, 128.80, 128.06, 125.97, 125.67, 119.46, 60.10, 50.25, 30.11, 29.67, 28.33, 26.13, 26.10. HRMS (FAB) calcd for $C_{20}H_{25}N_4OS$ $[M + H]^+$, 369.1749; found, 369.1762.

*1-(5-Azidopentyl)-3-methoxypyridin-2-one (**11**).* 3-Methoxypyridin-2-one (1.8g, 14.1 mmol) and 5-azidopentyl methanesulfonate **5d** (3.5g, 16.9 mmol) were dissolved in 2:1 (THF/MeOH) and stirred for 48 h at 80 °C. Upon completion of the reaction, EtOAc was added, and the organic layer was washed with H_2O and brine and dried to yield the crude product (2.42 g, 73%). The crude product was washed with petroleum ether, yielding **11** (1.96 g, 59%). ^{1}H NMR (400 MHz, $CDCl_3$) δ 6.74 (dd, J = 6.9, 1.6 Hz, 1H), 6.46 (dd, J = 7.4, 1.6 Hz, 1H), 5.95 (t, J = 7.1 Hz, 1H), 3.81 (t, J = 7.3 Hz, 2H), 3.64 (s, 3H), 3.11 (t, J = 6.8 Hz, 2H), 1.67−1.57 (m, 2H), 1.51−1.41 (m, 2H), 1.31−1.20 (m, 2H). ^{13}C NMR (101 MHz, $CDCl_3$) δ 157.46, 149.66, 127.87, 111.68, 104.34, 55.38, 50.72, 49.00, 28.14, 28.02, 23.28.

*3-Methoxy-1-(5-(4-(p-tolyl)-1H-1,2,3-triazol-1-yl)pentyl)pyridin-2-one (**12a**).* 1-Ethynyl-4-methylbenzene (0.14 g, 1.22 mmol) and **11** (0.24 g, 1.02 mmol) were dissolved in a 1:1 anhydrous THF/DMSO (10 mL) and stirred under argon at room temperature. Copper(I) iodide (0.01 g, 0.07 mmol) and Hunig's base (0.1 mL) were then added to the reaction mixture, and stirring was continued for 4 h. The reaction mixture was diluted with CH_2Cl_2 (40 mL) and washed with 1:4 NH_4OH/saturated NH_4Cl (3 × 30 mL) and saturated NH_4Cl (30 mL). The organic layer was dried over Na_2SO_4 and concentrated in vacuo. The crude product was purified by preparative TLC with 12:1 CH_2Cl_2/MeOH, resulting in **12a** (0.39 g, quantitative yield). ^{1}H NMR (400 MHz, cdcl$_3$) δ 7.69 (s, 1H), 7.58 (d, J = 8.2 Hz, 2H), 7.07 (d, J = 8.4 Hz, 2H), 6.70 (dd, J = 6.9, 1.6 Hz, 1H), 6.43 (dd, J = 7.4, 1.6 Hz, 1H), 5.92 (t, J = 7.1 Hz, 1H), 4.20 (t, J = 7.1 Hz, 2H), 3.77 (t, J = 7.2 Hz, 2H), 3.62 (s, 3H), 2.22 (s, 3H), 1.87−1.72 (m, 2H), 1.68−1.52 (m, 2H), 1.29−0.89 (m, 2H). ^{13}C NMR (101 MHz, cdcl$_3$) δ 157.77, 149.83, 147.52, 137.70, 129.38, 128.20, 127.80, 125.43, 119.54, 112.10, 104.80, 55.69, 49.81, 49.02, 29.57, 28.17, 23.14, 21.19.

*3-Methoxy-1-(5-(4-(m-tolyl)-1H-1,2,3-triazol-1-yl)pentyl)pyridin-2-one (**12b**).* 1-Ethynyl-3-methylbenzene (0.12 g, 1.05 mmol) and **11** (0.21 g, 0.88 mmol) were reacted as described for the synthesis of **12a** to give compound **12b** (0.3 g, 97%) as a yellow oil. ^{1}H NMR (400 MHz, $CDCl_3$) δ 7.74 (s, 1H), 7.59 (s, 1H), 7.52 (d, J = 7.7 Hz, 1H), 7.20 (t, J = 7.6 Hz, 1H), 7.04 (d, J = 7.6 Hz, 1H), 6.74 (dd, J = 6.9, 1.7 Hz, 1H), 6.48 (dd, J = 7.5, 1.6 Hz, 1H), 6.05−5.90 (m, 1H), 4.27 (t, J = 7.1 Hz, 2H), 3.83 (t, J = 7.2 Hz, 2H), 3.67 (s, 3H), 2.29 (s, 3H), 1.92−1.79 (m, 2H), 1.74−1.62 (m, 2H), 1.34−1.17 (m, 2H). ^{13}C NMR (101 MHz, $CDCl_3$) δ 157.53, 149.61, 147.34, 138.06, 130.18, 128.45, 128.34, 127.88, 125.94, 122.39, 119.49, 111.79, 104.55, 55.43, 49.58, 48.77, 29.31, 27.91, 22.87, 21.07.

*3-Methoxy-1-(5-(4-(o-tolyl)-1H-1,2,3-triazol-1-yl)pentyl)pyridin-2-one (**12c**).* 1-Ethynyl-2-methylbenzene (0.12 g, 1.06 mmol) and **11** (0.21 g, 0.89 mmol) were reacted as described for the synthesis of **12a** to give compound **12c** (0.21 g, 68%). ^{1}H NMR (400 MHz, $CDCl_3$) δ 7.72−7.62 (m, 1H), 7.61 (s, 1H), 7.16 (d, J = 3.1 Hz, 3H), 6.75 (dd, J = 6.9, 1.7 Hz, 1H), 6.48 (dd, J = 7.5, 1.6 Hz, 1H), 6.04−5.91 (m, 1H), 4.30 (t, J = 7.1 Hz, 2H), 3.85 (t, J = 7.2 Hz, 2H), 3.66 (s, 3H), 2.36 (s, 3H), 1.94−1.84 (m, 2H), 1.77−1.63 (m, 2H), 1.37−1.21 (m, 2H). ^{13}C NMR (101 MHz, $CDCl_3$) δ 157.89, 149.98, 146.89, 135.44, 130.81, 130.01, 128.78, 128.00, 125.99, 121.93, 112.14, 104.87, 55.76, 49.86, 49.12, 31.91, 29.67, 28.25, 23.26, 21.37.

*4-(1-(5-(3-Methoxy-2-oxopyridin-1(2H)-yl)pentyl)-1H-1,2,3-triazol-4-yl)benzonitrile (**12d**).* 4-Ethynylbenzonitrile (0.13 g, 1.05 mmol) and **11** (0.21 g, 0.87 mmol) were reacted as described for the synthesis of **12a** to give compound **12d** (0.30 g, 95%). ^{1}H NMR (400 MHz, $CDCl_3$) δ 7.96 (s, 1H), 7.81 (d, J = 8.7 Hz, 2H), 7.53 (d, J = 8.7 Hz, 2H), 6.73 (dd, J = 6.9, 1.7 Hz, 1H), 6.46 (dd, J = 7.5, 1.6 Hz, 1H), 5.98−5.90 (m, 1H), 4.28 (t, J = 7.1 Hz, 2H), 3.80 (t, J = 7.2 Hz, 2H), 3.62 (s, 3H), 1.90−1.77 (m, 2H), 1.71−1.59 (m, 2H), 1.31−1.15 (m, 2H). ^{13}C NMR (101 MHz, $CDCl_3$) δ 157.42, 149.48, 145.25, 134.76, 132.15, 127.79, 125.57, 120.99, 118.37, 111.83, 110.57, 104.52, 55.36, 49.63, 48.56, 29.04, 27.79, 22.71.

*3-(1-(5-(3-Methoxy-2-oxopyridin-1(2H)-yl)pentyl)-1H-1,2,3-triazol-4-yl)benzonitrile (**12e**).* 3-Ethynylbenzonitrile **16** (see the Supporting Information) (0.13 g, 1.05 mmol) and **11** (0.21 g, 0.87 mmol) were reacted as described for the synthesis of **12a** to give compound **12e** (0.31 g, 98%). ^{1}H NMR (400 MHz, $CDCl_3$) δ 8.01−7.97 (m, 1H), 7.96 (s, 1H), 7.94 (dt, J = 7.7, 1.5 Hz, 1H), 7.43 (dt, J = 7.7, 1.5 Hz, 1H), 7.38 (t, J = 7.5 Hz, 1H), 6.74 (dd, J = 6.9, 1.7 Hz, 1H), 6.46 (dd, J = 7.5, 1.6 Hz, 1H), 6.02−5.83 (m, 1H), 4.29 (t, J = 7.1 Hz, 2H), 3.80 (t, J = 7.2 Hz, 2H), 3.62 (s, 3H), 1.94−1.78 (m, 2H), 1.74−1.57 (m, 2H), 1.31−1.15 (m, 2H). ^{13}C NMR (101 MHz, $CDCl_3$) δ 157.74, 149.79, 145.29, 132.00, 131.09, 129.67, 129.60, 128.83, 128.14, 120.82, 118.50, 112.63, 112.14, 104.85, 55.68, 49.98, 48.93, 29.43, 28.14, 23.07.

*1-(5-(4-(4-(Dimethylamino)phenyl)-1H-1,2,3-triazol-1-yl)pentyl)-3-methoxypyridin-2-one (**12f**).* 4-Ethynyl-*N*,*N*-dimethylaniline (0.15 g, 1.02 mmol) and **11** (0.20 g, 0.85 mmol) were reacted as described for the synthesis of **12a** to give compound **12f** (0.27 g, 84%). ^{1}H NMR (400 MHz, $CDCl_3$) δ 7.55 (d, J = 2.4 Hz, 2H), 7.53 (s, 1H), 6.68 (d, J = 6.9 Hz, 1H), 6.59 (d, J = 9.0 Hz, 2H), 6.42 (d, J = 7.5 Hz, 1H), 5.93−5.87 (m, 1H), 4.15 (t, J = 7.1 Hz, 2H), 3.74 (t, J = 7.2 Hz, 2H), 3.60 (s, 3H), 2.80 (s, 6H), 1.81−1.71 (m, 2H), 1.64−1.53 (m, 2H), 1.22−1.07 (m, 2H). ^{13}C NMR (101 MHz, $CDCl_3$) δ 157.40, 149.82, 149.43, 147.58, 127.87, 126.10, 118.38, 117.97, 111.94, 111.81, 104.44, 55.32, 49.35, 48.68, 39.94, 29.19, 27.80, 22.78.

*4-(1-(5-(3-Methoxy-2-oxopyridin-1(2H)-yl)pentyl)-1H-1,2,3-triazol-4-yl)-2-(trifluoromethyl)benzonitrile (**12g**).* 4-Ethynyl-2-(trifluoromethyl)benzonitrile (0.09 g, 0.45 mmol) **18** (see the Supporting Information) and **11** (0.13 g, 0.54 mmol) were reacted as described for the synthesis of **12a** to give compound **12g** (0.19 g, 98%). ^{1}H NMR (400 MHz, $CDCl_3$) δ 8.25 (s, 1H), 8.12 (d, J = 5.2 Hz, 2H), 7.83 (d, J = 8.1 Hz, 1H), 6.81 (dd, J = 6.9, 1.5 Hz, 1H), 6.55 (dd, J = 7.4, 1.5 Hz, 1H), 6.06 (t, J = 7.1 Hz, 1H), 4.41 (t, J = 7.1 Hz, 2H), 3.91 (t, J = 7.2 Hz, 2H), 3.73 (d, J = 5.8 Hz, 3H), 2.07−1.91 (m, 2H), 1.83−1.68 (m, 2H), 1.41−1.27 (m, 2H). ^{13}C NMR (101 MHz, $CDCl_3$) δ 157.80, 149.88, 144.44, 135.56, 135.11, 128.51, 127.94, 123.40, 121.75, 120.79, 115.41, 111.99, 108.22, 104.87, 55.64, 50.05, 48.84, 29.25, 28.03, 23.55, 22.92.

*1-(4-Tolyl)triazolylpentyl-3-methoxypyridine-2-thione (**13a**).* A suspension of **12a** (0.24 g, 0.67 mmol) and Lawesson's reagent (0.16 g, 0.40 mmol) in toluene (12 mL) was heated at reflux for 12 h. The reaction mixture was cooled to room temperature, and the solvent was evaporated in vacuo. The crude solid was purified on preparative TLC, eluting with CH_2Cl_2/ acetone/MeOH (5:1:0.2) to give **13a** (0.23 g, 95%) as a yellow solid. ^{1}H NMR (400 MHz, $CDCl_3$) δ 7.77 (s, 1H), 7.73 (d, J = 8.2 Hz, 2H), 7.33 (m, 1H), 7.25 (dd, J = 11.4, 5.2

Hz, 2H), 6.66 (d, J = 7.8 Hz, 1H), 6.59 (dd, J = 7.8, 6.5 Hz, 1H), 4.60 (m, 2H), 4.43 (t, J = 6.9 Hz, 2H), 3.91 (s, 3H), 2.38 (s, 3H), 2.01 (m, 4H), 1.43 (m, 2H). ^{13}C NMR (75 MHz, $CDCl_3$) δ 171.03, 158.50, 147.11, 137.37, 131.77, 129.02, 127.33, 125.03, 119.32, 111.60, 109.78, 56.27, 49.28, 30.48, 29.05, 26.51, 22.57, 20.82. HRMS (EI) calcd for $C_{20}H_{24}N_4OS$ $[M]^+$, 368.1671; found, 368.1667.

*1-(3-Tolyl)triazolylpentyl-3-methoxypyridine-2-thione (**13b**).* Reaction of **12b** (0.14 g, 0.39 mmol) and Lawesson's reagent (0.09 g, 0.22 mmol) in toluene (10 mL) within 12 h as described for the synthesis of **13a** gave compound **13b** (0.10 g, 73%) as a yellow solid. ^{1}H NMR (400 MHz, $CDCl_3$) δ 7.78 (s, 1H), 7.62 (s, 1H), 7.54 (d, J = 7.7 Hz, 1H), 7.26 (m, 2H), 7.07 (d, J = 7.6 Hz, 1H), 6.59 (m, 1H), 6.52 (dd, J = 7.8, 6.5 Hz, 1H), 4.50 (m, 2H), 4.34 (t, J = 7.0 Hz, 2H), 3.81 (s, 3H), 2.32 (s, 3H), 1.90 (m, 4H), 1.33 (m, 2H). ^{13}C NMR (100 MHz, $CDCl_3$) δ 171.47, 158.81, 147.45, 138.19, 131.83, 130.21, 128.58, 128.46, 126.03, 122.48, 119.68, 111.72, 109.80, 56.55, 56.47, 49.50, 29.24, 26.70, 22.77, 21.18. HRMS (EI) calcd for $C_{20}H_{24}N_4OS$ $[M]^+$, 368.1671; found, 368.1682.

*1-(2-Tolyl)triazolylpentyl-3-methoxypyridine-2-thione (**13c**).* Reaction of **12c** (0.12 g, 0.35 mmol) and Lawesson's reagent (0.09 g, 0.21 mmol) in toluene (10 mL) within 12 h as described for the synthesis of **13a** gave compound **13c** (0.09 g, 72%) as a yellow solid. ^{1}H NMR (400 MHz, $CDCl_3$) δ 7.72 (m, 1H), 7.27 (m, 2H), 6.60 (m, 1H), 4.57 (m, 1H), 4.42 (t, J = 7.0 Hz, 1H), 3.86 (s, 1H), 2.44 (s, 1H), 1.99 (m, 2H), 1.41 (dt, J = 15.2, 7.6 Hz, 1H). ^{13}C NMR (100 MHz, $CDCl_3$) δ 171.81, 159.04, 146.84, 135.33, 131.86, 130.74, 129.81, 128.68, 127.94, 125.93, 121.86, 111.78, 109.79, 104.88, 56.75, 56.61, 49.60, 29.45, 26.85, 22.97, 21.36. HRMS (EI) calcd for $C_{20}H_{24}N_4OS$ $[M]^+$, 368.1671; found, 368.1662.

*1-(4-Benzonitrile)triazolylpentyl-3-methoxypyridine-2-thione (**13d**).* Reaction of **12d** (0.21 g, 0.55 mmol) and Lawesson's reagent (0.13 g, 0.33 mmol) in toluene (12 mL) within 12 h as described for the synthesis of **13a** gave compound **13d** (0.15 g, 67%) as a yellow solid. ^{1}H NMR (400 MHz, $CDCl_3$) δ 7.64 (m, 3H), 7.28 (m, 1H), 6.73 (d, J = 8.3 Hz, 2H), 6.61 (d, J = 7.6 Hz, 1H), 6.52 (t, J = 7.1 Hz, 1H), 4.50 (m, 2H), 4.31 (t, J = 6.7 Hz, 2H), 3.81 (s, 3H), 2.92 (s, 6H), 1.89 (m, 4H), 1.32 (m, 2H). ^{13}C NMR (100 MHz, $CDCl_3$) δ 171.44, 158.81, 149.78, 147.77, 131.91, 126.37, 119.05, 118.34, 112.52, 111.73, 109.84, 56.60, 56.49, 49.44, 40.45, 29.29, 26.74, 22.81. HRMS (EI) calcd for $C_{20}H_{21}N_5OS$ $[M]^+$, 379.1467; found, 379.1469.

*1-(3-Benzonitrile)triazolylpentyl-3-methoxypyridine-2-thione (**13e**).* Reaction of **12e** (0.19 g, 0.52 mmol) and Lawesson's reagent (0.13 g, 0.31 mmol) in toluene (10 mL) within 12 h as described for the synthesis of **13a** gave compound **13e** (0.13 g, 67%) as a yellow solid. ^{1}H NMR (400 MHz, $CDCl_3$) δ 7.98 (s, 1H), 7.84 (d, J = 8.4 Hz, 2H), 7.56 (d, J = 8.4 Hz, 2H), 7.30 (d, J = 6.5 Hz, 1H), 6.60 (d, J = 7.0 Hz, 1H), 6.52 (dd, J = 7.7, 6.6 Hz, 1H), 4.48 (m, 2H), 4.34 (t, J = 6.9 Hz, 2H), 3.76 (s, 3H), 1.88 (m, 4H), 1.31 (m, 2H). ^{13}C NMR (100 MHz, $CDCl_3$) δ 171.23, 158.70, 145.36, 134.76, 132.30, 131.78, 125.68, 121.20, 118.49, 111.83, 110.73, 109.92, 56.43, 49.50, 29.01, 26.56, 22.56. HRMS (EI) calcd for $C_{20}H_{21}N_5OS$ $[M]^+$, 379.1467; found, 379.1466.

*1-(4-(N,N-Dimethylaniline))triazolylpentyl-3-methoxypyridine-2-thione (**13f**).* Reaction of **12f** (0.15 g, 0.40 mmol) and Lawesson's reagent (0.10 g, 0.24 mmol) in toluene (10 mL) within 12 h as described for the synthesis of **13a** gave compound **13f** (0.15 g, 98%) as a yellow solid. ^{1}H NMR (400 MHz, $CDCl_3$) δ 8.12 (t, J = 1.4 Hz, 1H), 8.06 (m, 1H), 7.90 (s, 1H), 7.59 (dt, J = 7.7, 1.4 Hz, 1H), 7.52 (t, J = 7.8 Hz, 1H), 7.33 (dd, J = 6.5, 1.4 Hz, 1H), 6.67 (dd, J = 7.9, 1.3 Hz, 1H), 6.60 (dd, J = 7.8, 6.5 Hz, 1H), 4.59 (m, 2H), 4.46 (t, J = 6.9 Hz, 2H), 3.89 (s, 3H), 2.02 (m, 4H), 1.43 (m, 2H). ^{13}C NMR (100 MHz, $CDCl_3$) δ 171.30, 158.73, 145.13, 131.82, 131.71, 130.97, 129.52, 129.44, 128.64, 120.61, 118.28, 112.49, 111.81, 109.91, 56.44, 49.62, 29.11, 26.64, 22.68. HRMS (EI) calcd for $C_{21}H_{27}N_5OS$ $[M]^+$, 397.1936; found, 397.1928.

*1-(4-(3-Trifluomethyl)-benzonitrile)triazolylpentyl-3-methoxypyridine-2-thione (**13g**).* Reaction of **12g** (0.09 g, 0.21 mmol) and Lawesson's reagent (0.05 g, 0.13 mmol) in toluene (10 mL) within 12 h as described for the synthesis of **13a** gave compound **13g** (0.08 g, 81%) as a yellow solid. ^{1}H NMR (400 MHz, $CDCl_3$) δ 8.28 (s, 1H), 8.12 (d, J = 6.7 Hz, 2H), 7.86 (d, J = 8.1 Hz, 1H), 7.36 (d, J = 6.5 Hz, 1H), 6.68 (d, J = 7.8 Hz, 1H), 6.61 (t, J = 7.2 Hz, 1H), 4.59 (m, 2H), 4.47 (m, 2H), 3.88 (s, 3H), 2.02 (m, 4H), 1.43 (m, 2H). ^{13}C NMR (100 MHz, $CDCl_3$) δ 171.84, 159.14, 144.54, 135.55, 135.22, 133.51, 133.18, 131.81, 128.59, 121.86, 120.86, 115.46, 112.00, 109.97, 108.47, 77.31, 76.99, 76.67, 56.69, 49.87, 29.19, 26.77, 22.77. HRMS (EI) calcd for $C_{21}H_{20}N_5OSF_3$ $[M]^+$, 447.1341; found, 447.1341.

*1-(4-Tolyl)triazolylpentyl-3-hydroxypyridine-2-thione (**14a**).* Reaction of **13a** (0.08 g, 0.20 mmol) and 1 M BBr_3 (0.24 mL) in CH_2Cl_2 (8 mL) within 48 h as described for the synthesis of **10a** gave compound **14a** (0.04 g, 62%) as an olive green solid. t_R 11.0 min. ^{1}H NMR (400 MHz, CD_3OD) δ 8.18 (s, 1H), 7.66 (d, J = 8.0 Hz, 2H), 7.55 (d, J = 5.7 Hz, 1H), 7.20 (d, J = 7.7 Hz, 2H), 6.97 (d, J = 6.7 Hz, 1H), 4.55 (m, 2H), 4.43 (t, J = 6.7 Hz, 2H), 2.34 (s, 3H), 2.01 (m, 4H), 1.39 (t, J = 22.5 Hz, 2H). ^{13}C NMR (100 MHz, CD_3OD) δ 149.25, 139.68, 130.93, 129.13, 127.01, 122.27, 51.41, 30.95, 24.51, 21.83. HRMS (EI) calcd for $C_{19}H_{22}N_4OS$ $[M]^+$, 354.1514; found, 354.1512.

*1-(3-Tolyl)triazolylpentyl-3-hydroxypyridine-2-thione (**14b**).* Reaction of **13b** (0.10 g, 0.27 mmol) and 1 M BBr_3 (0.33 mL) in CH_2Cl_2 (8 mL) within 48 h as described for the synthesis of **10a** gave compound **14b** (0.05 g, 56%) as an olive green solid. t_R 11.1 min. ^{1}H NMR (400 MHz, CD_3OD) δ 8.20 (s, 1H), 7.61 (s, 1H), 7.55 (m, 2H), 7.26 (t, J = 7.6 Hz, 1H), 7.12 (d, J = 7.5 Hz, 1H), 6.92 (m, 2H), 4.55 (m, 2H), 4.44 (t, J = 6.7 Hz, 2H), 2.36 (s, 3H), 2.01 (m, 4H), 1.41 (m, 2H). ^{13}C NMR (100 MHz, CD_3OD) δ 149.29, 140.05, 131.87, 131.78, 130.38, 130.20, 127.90, 127.63, 124.13, 122.51, 51.40, 31.07, 30.93, 28.97, 24.49, 22.02. HRMS (EI) calcd for $C_{19}H_{22}N_4OS$ $[M]^+$, 354.1514; found, 354.1523.

*1-(2-Tolyl)triazolylpentyl-3-hydroxypyridine-2-thione (**14c**).* Reaction of **13c** (0.07 g, 0.20 mmol) and 1 M BBr_3 (0.30 mL) in CH_2Cl_2 (8 mL) within 48 h as described for the synthesis of **10a** gave compound **14c** (0.05 g, 67%) as an olive green solid. t_R 10.6 min. ^{1}H NMR (400 MHz, CD_3OD) δ 7.94 (s, 1H), 7.61 (m, 1H), 7.47 (s, 1H), 7.21 (m, 1H), 6.97 (m, 1H), 6.76 (m, 1H), 4.52 (m, 1H), 4.45 (t, J = 6.8 Hz, 1H), 2.38 (s, 1H), 2.01 (m, 2H), 1.43 (m, 1H). ^{13}C NMR (100 MHz, CD_3OD) δ 146.74, 135.53, 130.65, 129.46, 128.69, 128.21, 125.88, 122.79, 53.41, 49.83, 29.42, 27.32, 22.98, 20.55. HRMS (EI) calcd for $C_{19}H_{22}N_4OS$ $[M]^+$, 354.1514; found, 354.1509.

*1-(4-Benzonitrile)triazolylpentyl-3-hydroxypyridine-2-thione (**14d**).* Reaction of **13d** (0.10 g, 0.271 mmol) and 1 M BBr_3 (0.33 mL) in CH_2Cl_2 (8 mL) within 48 h as described for the synthesis of **10a** gave compound **14d** (0.053 g, 56%) as an olive green solid. t_R 9.4 min. ^{1}H NMR (400 MHz, DMSO-d_6) δ 8.53 (s, 1H), 8.27 (s, 1H), 7.82 (d, J = 7.1 Hz, 1H), 7.62 (d, J = 8.8 Hz, 2H), 7.06 (d, J = 7.5 Hz, 1H), 6.93 (m, 1H), 6.77 (m, 2H), 4.52 (d, J = 6.9 Hz, 2H), 4.36 (t, J = 7.0 Hz, 2H), 3.21 (s, 6H), 1.88 (m, 4H), 1.34 (m, 2H). ^{13}C NMR (100 MHz, CD_3OD) δ 145.3, 132.0, 131.1, 129.7, 129.6, 128.6, 121.7, 112.7, 105.0, 49.8, 29.1, 27.0, 22.7. HRMS (EI) calcd for $C_{19}H_{19}N_5OS$ $[M]^+$, 365.1310; found, 365.1310.

*1-(3-Benzonitrile)triazolylpentyl-3-hydroxypyridine-2-thione (**14e**).* Reaction of **13e** (0.10 g, 0.25 mmol) and 1 M BBr_3 (0.30 mL) in CH_2Cl_2 (8 mL) within 48 h as described for the synthesis of **10a** gave compound **14e** (0.06 g, 60%) as an olive green solid. t_R 9.3 min. ^{1}H NMR (400 MHz, DMSO) δ 8.76 (s, 1H), 8.01 (d, J = 8.1 Hz, 2H), 7.87 (m, 2H), 7.65 (d, J = 6.4 Hz, 1H), 7.00 (m, 1H), 6.87 (d, J = 8.2 Hz, 1H), 6.70 (m, 1H), 4.44 (m, 4H), 1.89 (m, 4H), 1.31 (m, 2H). ^{13}C NMR (100 MHz, $CDCl_3$) δ 168.23, 155.01, 145.75, 134.86, 132.56, 131.00, 125.91, 121.05, 118.68, 113.76, 112.04, 111.17, 57.64, 49.81, 29.31, 27.06, 22.91. HRMS (EI) calcd for $C_{19}H_{19}N_5OS$ $[M]^+$, 365.1310; found, 365.1313.

*1-(4-(N,N-Dimethylaniline)triazolylpentyl-3-hydroxypyridine-2-thione (**14f**).* Reaction of **13f** (0.11 g, 0.25 mmol) and 1 M BBr_3 (0.33 mL) in CH_2Cl_2 (8 mL) within 48 h as described for the synthesis of **10a** gave compound **14f** (0.07 g, 66%) as an olive green solid. t_R 4.6 min. ^{1}H NMR (400 MHz, CD_3OD) δ 8.38 (s, 1H), 8.15 (s, 1H), 8.10 (d, J = 7.9 Hz, 1H), 7.63 (m, 3H), 6.95 (d, J = 7.5 Hz, 1H), 6.67 (m, 1H), 4.57 (m, 2H), 4.48 (t, J = 7.0 Hz, 2H), 2.03 (m, 4H), 1.43 (m, 2H). ^{13}C NMR (100 MHz, CD_3OD) δ 145.34, 132.04, 131.14, 129.72,

dx.doi.org/10.1021/jm401225q | J. Med. Chem. 2013, 56, 9969−9981

129.58, 128.63, 121.75, 112.74, 104.99, 49.79, 29.08, 27.04, 22.73. HRMS (EI) calcd for $C_{20}H_{25}N_5OS$ $[M]^+$, 383.1780; found, 383.1776.

*1-(4-(3-Trifluomethyl)-benzonitrile)triazolylpentyl-3-hydroxypyridine-2-thione (**14g**).* Reaction of **13g** (0.11 g, 0.25 mmol) and 1 M BBr_3 (0.33 mL) in CH_2Cl_2 (8 mL) within 48 h as described for the synthesis of **10a** gave compound **14g** (0.072 g, 66%) as an olive green solid. t_R 12.4 min. ^{1}H NMR (400 MHz, CD_3OD) δ 8.59 (s, 1H), 8.35 (s, 1H), 8.21 (d, J = 7.8 Hz, 1H), 8.00 (t, J = 9.5 Hz, 1H), 7.58 (d, J = 6.2 Hz, 1H), 6.96 (d, J = 7.5 Hz, 1H), 6.72 (m, 1H), 4.57 (m, 4H), 2.04 (m, 4H), 1.42 (m, 2H). ^{13}C NMR (100 MHz, CD_3OD) δ 146.09, 137.48, 137.24, 134.79, 130.46, 125.55, 124.87, 123.60, 122.77, 116.84, 109.75, 55.10, 51.63, 30.84, 28.90, 24.47. HRMS (EI) calcd for $C_{19}H_{19}N_5OS$ $[M]^+$, 365.1310; found, 365.1310. HRMS (EI) calcd for $C_{20}H_{18}N_5OS$ $[M]^+$, 433.1184; found, 433.1189.

*1-(4-Tolyl)triazolylpentyl-3-hydroxypyridin-2-one (**15a**).* Reaction of **12a** (0.10 g, 0.28 mmol) and 1 M BBr_3 (0.34 mL) in CH_2Cl_2 (8 mL) within 48 h as described for the synthesis of **10a** gave compound **15a** (0.05 g, 52%) as a light brown solid. ^{1}H NMR (400 MHz, $CDCl_3$) δ 7.71 (m, 3H), 7.24 (m, 2H), 6.76 (t, J = 6.4 Hz, 2H), 6.12 (t, J = 7.0 Hz, 1H), 4.40 (t, J = 6.9 Hz, 2H), 3.96 (t, J = 7.1 Hz, 2H), 2.38 (s, 3H), 2.00 (m, 2H), 1.82 (m, 2H), 1.39 (m, 2H). ^{13}C NMR (100 MHz, DMSO) δ 171.80, 146.31, 137.02, 129.40, 128.08, 125.02, 120.79, 114.36, 105.20, 49.27, 48.22, 29.17, 28.01, 22.85, 20.82. HRMS (EI) calcd for $C_{19}H_{22}N_4O_2$ $[M]^+$, 338.1743; found, 338.1750.

*1-(3-Tolyl)triazolylpentyl-3-hydroxypyridin-2-one (**15b**).* Reaction of **12b** (0.07 g, 0.21 mmol) and 1 M BBr_3 (0.24 mL) in CH_2Cl_2 (8 mL) within 48 h as described for the synthesis of **10a** gave compound **15b** (0.05 g, 74%) as a light brown solid. ^{1}H NMR (400 MHz, $CDCl_3$) δ 7.74 (s, 1H), 7.67 (s, 1H), 7.59 (d, J = 7.7 Hz, 1H), 7.30 (t, J = 7.6 Hz, 1H), 7.14 (d, J = 7.4 Hz, 1H), 6.76 (t, J = 6.2 Hz, 2H), 6.12 (t, J = 7.1 Hz, 1H), 4.39 (t, J = 6.9 Hz, 2H), 3.96 (t, J = 7.2 Hz, 2H), 2.39 (s, 3H), 1.99 (m, 2H), 1.80 (m, 2H), 1.38 (m, 2H). ^{13}C NMR (100 MHz, $CDCl_3$) δ 158.58, 147.87, 146.52, 138.46, 130.38, 128.86, 128.67, 126.75, 126.31, 122.72, 119.48, 113.61, 106.85, 49.91, 49.45, 29.65, 28.38, 23.27, 21.38. HRMS (EI) calcd for $C_{19}H_{22}N_4O_2$ $[M]^+$, 338.1743; found, 338.1741.

*1-(2-Tolyl)triazolylpentyl-3-hydroxypyridin-2-one (**15c**).* Reaction of **12c** (0.07 g, 0.18 mmol) and 1 M BBr_3 (0.27 mL) in CH_2Cl_2 (8 mL) within 48 h as described for the synthesis of **10a** gave compound **15c** (0.05 g, 87%) as a light brown solid. ^{1}H NMR (400 MHz, dmso) δ 8.92 (s, 1H), 8.36 (s, 1H), 7.71 (m, 1H), 7.25 (m, 1H), 7.09 (d, J = 6.8 Hz, 1H), 6.64 (d, J = 6.9 Hz, 1H), 6.04 (t, J = 7.0 Hz, 1H), 4.39 (t, J = 6.9 Hz, 1H), 3.88 (t, J = 7.0 Hz, 1H), 2.41 (s, 1H), 1.90 (m, 1H), 1.67 (m, 1H), 1.25 (m, 1H). ^{13}C NMR (100 MHz, CD_3OD) δ 146.28, 135.00, 130.15, 128.96, 128.21, 127.72, 125.38, 122.09, 106.72, 49.43, 48.98, 29.05, 27.78, 22.69, 20.09. HRMS (EI) calcd for $C_{19}H_{22}N_4O_2$ $[M]^+$, 338.1743; found, 338.1741.

*1-(4-Benzonitrile)triazolylpentyl-3-hydroxypyridin-2-one (**15d**).* Reaction of **12d** (0.08 g, 0.20 mmol) and 1 M BBr_3 (0.24 mL) in CH_2Cl_2 (8 mL) within 48 h as described for the synthesis of **10a** gave compound **15d** (0.04 g, 60%) as a light brown solid. ^{1}H NMR (400 MHz, $CDCl_3$) δ 7.69 (d, J = 8.8 Hz, 2H), 7.61 (s, 1H), 6.77 (m, 4H), 6.11 (t, J = 7.1 Hz, 1H), 4.37 (t, J = 6.9 Hz, 2H), 3.96 (t, J = 7.2 Hz, 2H), 2.99 (s, 6H), 1.99 (m, 2H), 1.81 (m, 2H), 1.39 (m, 2H). ^{13}C NMR (100 MHz, $CDCl_3$) δ 158.57, 150.35, 148.26, 146.61, 126.84, 126.61, 118.87, 118.11, 113.72, 112.49, 106.86, 49.83, 49.52, 40.46, 29.70, 28.41, 23.34. HRMS (EI) calcd for $C_{19}H_{19}N_5O_2$ $[M]^+$, 349.1539; found, 349.1539.

*1-(3-Benzonitrile)triazolylpentyl-3-hydroxypyridin-2-one (**15e**).* Reaction of **12e** (0.09 g, 0.25 mmol) and 1 M BBr_3 (0.30 mL) in CH_2Cl_2 (8 mL) within 48 h as described for the synthesis of **10a** gave compound **15e** (0.06 g, 72%) as a light brown solid. ^{1}H NMR (400 MHz, DMSO) δ 8.93 (s, 1H), 8.76 (s, 1H), 8.01 (d, J = 7.7 Hz, 2H), 7.90 (d, J = 8.0 Hz, 2H), 7.09 (d, J = 6.4 Hz, 1H), 6.64 (d, J = 7.1 Hz, 1H), 6.04 (t, J = 7.0 Hz, 1H), 4.41 (t, J = 6.5 Hz, 2H), 3.88 (t, J = 6.9 Hz, 2H), 1.89 (m, 2H), 1.67 (m, 2H), 1.24 (m, 2H). ^{13}C NMR (100 MHz, $CDCl_3$) δ 146.62, 145.80, 134.92, 132.57, 126.69, 125.93, 120.88, 118.70, 114.06, 111.19, 107.06, 50.00, 49.29, 29.43, 28.28, 23.08. HRMS (EI) calcd for $C_{19}H_{19}N_5O_2$ $[M]^+$, 349.1539; found, 349.1544.

*1-(4-(N,N-Dimethylaniline))triazolylpentyl-3-hydroxypyridin-2-one (**15f**).* Reaction of **12f** (0.08 g, 0.22 mmol) and 1 M BBr_3 (0.26 mL) in CH_2Cl_2 (6 mL) within 48 h as described for the synthesis of **10a** gave compound **15f** (0.05 g, 64%) as a light brown solid. ^{1}H NMR (400 MHz, CD_3OD) δ 8.39 (s, 1H), 8.16 (s, 1H), 8.12 (d, J = 7.5 Hz, 1H), 7.68 (d, J = 7.5 Hz, 1H), 7.61 (t, J = 7.6 Hz, 1H), 7.04 (m, 1H), 6.76 (m, 1H), 6.21 (m, 1H), 4.45 (m, 2H), 3.99 (m, 2H), 2.01 (m, 2H), 1.78 (m, 2H), 1.33 (m, 2H). ^{13}C NMR (100 MHz, $CDCl_3$) δ 145.61, 131.97, 131.31, 129.74, 129.65, 129.10, 120.30, 118.49, 112.99, 104.90, 50.07, 49.40, 29.52, 28.37, 23.17. HRMS (EI) calcd for $C_{20}H_{25}N_5O_2$ $[M]^+$, 367.2008; found, 367.2007.

*1-(4-(3-Trifluomethyl)-benzonitrile)triazolylpentyl-3-hydroxypyridin-2-one (**15g**).* Reaction of **12g** (0.04 g, 0.10 mmol) and 1 M BBr_3 (0.17 mL) in CH_2Cl_2 (6 mL) within 48 h as described for the synthesis of **10a** gave compound **15g** (0.04 g, 85%) as a light brown solid. ^{1}H NMR (400 MHz, $CDCl_3$) δ 8.24 (s, 1H), 8.12 (d, J = 7.9 Hz, 1H), 8.00 (s, 1H), 7.86 (d, J = 7.9 Hz, 1H), 6.75 (t, J = 5.8 Hz, 2H), 6.12 (t, J = 7.0 Hz, 1H), 4.44 (t, J = 6.9 Hz, 2H), 3.96 (t, J = 7.1 Hz, 2H), 2.02 (m, 2H), 1.81 (m, 2H), 1.37 (m, 2H). ^{13}C NMR (100 MHz, $CDCl_3$) δ 158.58, 146.54, 144.71, 135.49, 135.26, 128.57, 126.70, 123.59, 123.54, 121.46, 115.47, 113.82, 108.63, 107.02, 50.19, 49.31, 29.45, 28.30, 23.12. HRMS (EI) calcd for $C_{20}H_{18}N_5O_2F_3$ $[M]^+$, 417.1413; found, 417.1425.

■ ASSOCIATED CONTENT

Ⓢ Supporting Information

^{1}H and ^{13}C NMR spectral information, solubility data, and molecular modeling. This material is available free of charge via the Internet at http://pubs.acs.org.

■ AUTHOR INFORMATION

Corresponding Authors

*(M.M.) E-mail: milan.mrksich@northwestern.edu. Phone: 847-467-0472. Fax: 847-467-3057.

*(A.K.O.) E-mail: aoyelere@gatech.edu. Phone: 404-894-4047. Fax: 404-894-2291.

Author Contributions

‖These authors contributed equally to this work.

Notes

The authors declare no competing financial interest.

■ ACKNOWLEDGMENTS

We are grateful to Professor Olaf Wiest for providing us with the HDAC 1 homology model. This work was financially supported by NIH grant R01CA131217 (A.K.O.) and R01GM084188 (M.M.). Q.H.S. is a recipient of a Southern Regional Education Board Dissertation Fellowship and a GAANN predoctoral fellowship from the Georgia Tech Center for Drug Design, Development, and Delivery. We are grateful to the ACS for a Division of Medicinal Chemistry travel award to V.P.

■ ABBREVIATION USED

HDAC, histone deacetylase; HDACi, histone deacetylase inhibitors; ZBG, zinc binding group; TSA, trichostatin A; 3HPT, 3-hydroxypyridine-2-thione; MMP, matrix metalloproteinase; CTCL, cutaneous T-cell lymphoma

■ REFERENCES

(1) Minucci, S.; Pelicci, P. G. Histone deacetylase inhibitors and the promise of epigenetic (and more) treatments for cancer. *Nat. Rev. Cancer* **2006**, *6*, 38−51.

(2) Jain, S.; Zain, J.; O'Connor, O. Novel therapeutic agents for cutaneous T-cell lymphoma. *J. Hematol. Oncol.* **2012**, *5*, 24.

(3) Gryder, B. E.; Sodji, Q. H.; Oyelere, A. K. Targeted cancer therapy: Giving histone deacetylase inhibitors all they need to succeed. *Future Med. Chem.* **2012**, *4*, 505−524.
(4) Kontogiorgis, C. A.; Papaioannou, P.; Hadjipavlou-Litina, D. J. Matrix metalloproteinase inhibitors: A review on pharmacophore mapping and (Q)SARs results. *Curr. Med. Chem.* **2005**, *12*, 339−355.
(5) Botta, C. B.; Cabri, W.; Cini, E.; De Cesare, L.; Fattorusso, C.; Giannini, G.; Persico, M.; Petrella, A.; Rondinelli, F.; Rodriquez, M.; Russo, A.; Taddei, M. Oxime amides as a novel zinc binding group in histone deacetylase inhibitors: Synthesis, biological activity, and computational evaluation. *J. Med. Chem.* **2011**, *54*, 2165−2182.
(6) Suzuki, T.; Ando, T.; Tsuchiya, K.; Fukazawa, N.; Saito, A.; Mariko, Y.; Yamashita, T.; Nakanishi, O. Synthesis and histone deacetylase inhibitory activity of new benzamide derivatives. *J. Med. Chem.* **1999**, *42*, 3001−3003.
(7) Suzuki, T.; Nagano, Y.; Matsuura, A.; Kohara, A.; Ninomiya, S.-i.; Kohda, K.; Miyata, N. Novel histone deacetylase inhibitors: Design, synthesis, enzyme inhibition, and binding mode study of SAHA-based non-hydroxamates. *Bioorg. Med. Chem. Lett.* **2003**, *13*, 4321−4326.
(8) Chen, B.; Petukhov, P. A.; Jung, M.; Velena, A.; Eliseeva, E.; Dritschilo, A.; Kozikowski, A. P. Chemistry and biology of mercaptoacetamides as novel histone deacetylase inhibitors. *Bioorg. Med. Chem. Lett.* **2005**, *15*, 1389−1392.
(9) Patil, V.; Sodji, Q. H.; Kornacki, J. R.; Mrksich, M.; Oyelere, A. K. 3-Hydroxypyridin-2-thione as novel zinc binding group for selective histone deacetylase inhibition. *J. Med. Chem.* **2013**, *56*, 3492−3506.
(10) Chen, P. C.; Patil, V.; Guerrant, W.; Green, P.; Oyelere, A. K. Synthesis and structure-activity relationship of histone deacetylase (HDAC) inhibitors with triazole-linked cap group. *Bioorg. Med. Chem.* **2008**, *16*, 4839−4853.
(11) Rostovtsev, V. V.; Green, L. G.; Fokin, V. V.; Sharpless, K. B. A stepwise Huisgen cycloaddition process: Copper(I)-catalyzed regioselective "ligation" of azides and terminal alkynes. *Angew. Chem., Int. Ed.* **2002**, *41*, 2596−2599.
(12) Tornøe, C. W.; Christensen, C.; Meldal, M. Peptidotriazoles on solid phase: [1,2,3]-Triazoles by regiospecific copper(I)-catalyzed 1,3-dipolar cycloadditions of terminal alkynes to azides. *J. Org. Chem.* **2002**, *67*, 3057−3064.
(13) Ozturk, T.; Ertas, E.; Mert, O.; Berzelius, A. Reagent, phosphorus decasulfide (P_4S_{10}), in organic syntheses. *Chem. Rev.* **2010**, *110*, 3419−3478.
(14) Brayton, D.; Jacobsen, F. E.; Cohen, S. M.; Farmer, P. J. A novel heterocyclic atom exchange reaction with Lawesson's reagent: A one-pot synthesis of dithiomaltol. *Chem. Commun.* **2006**, *0*, 206−208.
(15) Mwakwari, S. C.; Guerrant, W.; Patil, V.; Khan, S. I.; Tekwani, B. L.; Gurard-Levin, Z. A.; Mrksich, M.; Oyelere, A. K. Non-peptide macrocyclic histone deacetylase inhibitors derived from tricyclic ketolide skeleton. *J. Med. Chem.* **2010**, *53*, 6100−6111.
(16) Gurard-Levin, Z. A.; Mrksich, M. The activity of HDAC8 depends on local and distal sequences of its peptide substrates. *Biochemistry* **2008**, *47*, 6242−6250.
(17) Gurard-Levin, Z. A.; Scholle, M. D.; Eisenberg, A. H.; Mrksich, M. High-throughput screening of small molecule libraries using SAMDI mass spectrometry. *ACS Comb. Sci.* **2011**, *13*, 347−350.
(18) Di Micco, S.; Chini, M. G.; Terracciano, S.; Bruno, I.; Riccio, R.; Bifulco, G. Structural basis for the design and synthesis of selective HDAC inhibitors. *Bioorg. Med. Chem.* **2013**, *21*, 3795−3807.
(19) Butler, K. V.; Kalin, J.; Brochier, C.; Vistoli, G.; Langley, B.; Kozikowski, A. P. Rational design and simple chemistry yield a superior, neuroprotective HDAC6 inhibitor, tubastatin A. *J. Am. Chem. Soc.* **2010**, *132*, 10842−10846.
(20) Whitehead, L.; Dobler, M. R.; Radetich, B.; Zhu, Y.; Atadja, P. W.; Claiborne, T.; Grob, J. E.; McRiner, A.; Pancost, M. R.; Patnaik, A.; Shao, W.; Shultz, M.; Tichkule, R.; Tommasi, R. A.; Vash, B.; Wang, P.; Stams, T. Human HDAC isoform selectivity achieved via exploitation of the acetate release channel with structurally unique small molecule inhibitors. *Bioorg. Med. Chem.* **2011**, *19*, 4626−4634.
(21) Balasubramanian, S.; Ramos, J.; Luo, W.; Sirisawad, M.; Verner, E.; Buggy, J. J. A novel histone deacetylase 8 (HDAC8)-specific inhibitor PCI-34051 induces apoptosis in T-cell lymphomas. *Leukemia* **2008**, *22*, 1026−1034.
(22) Aldana-Masangkay, G. I.; Sakamoto, K. M., The Role of HDAC6 in Cancer. *J. Biomed. Biotechnol.* **2011**, *2011*.
(23) Yamaki, H.; Nakajima, M.; Shimotohno, K. W.; Tanaka, N. Molecular basis for the actions of Hsp90 inhibitors and cancer therapy. *J. Antibiot.* **2011**, *64*, 635−644.
(24) Williams, C. R.; Tabios, R.; Linehan, W. M.; Neckers, L. Intratumor Injection of the Hsp90 Inhibitor 17AAG Decreases Tumor Growth and Induces Apoptosis in a Prostate Cancer Xenograft Model. *J. Urol.* **2007**, *178*, 1528−1532.
(25) Namdar, M.; Perez, G.; Ngo, L.; Marks, P. A. Selective inhibition of histone deacetylase 6 (HDAC6) induces DNA damage and sensitizes transformed cells to anticancer agents. *Proc. Natl. Acad. Sci. U.S.A.* **2010**, *107*, 20003−20008.
(26) Hackanson, B.; Rimmele, L.; Benkißer, M.; Abdelkarim, M.; Fliegauf, M.; Jung, M.; Lübbert, M. HDAC6 as a target for antileukemic drugs in acute myeloid leukemia. *Leuk. Res.* **2012**, *36*, 1055−1062.
(27) Lipinski, C. A.; Lombardo, F.; Dominy, B. W.; Feeney, P. J. Experimental and computational approaches to estimate solubility and permeability in drug discovery and development settings. *Adv. Drug Delivery Rev.* **1997**, *23*, 3−25.
(28) Kerns, E. H.; Di, L.; Carter, G. T. In vitro solubility assays in drug discovery. *Curr. Drug Metab.* **2008**, *9*, 879−885.
(29) Shalinsky, D. R.; Brekken, J.; Zou, H.; McDermott, C. D.; Forsyth, P.; Edwards, D.; Margosiak, S.; Bender, S.; Truitt, G.; Wood, A.; Varki, N. M.; Appelt, K. Broad Antitumor and Antiangiogenic Activities of AG3340, a Potent and Selective MMP Inhibitor Undergoing Advanced Oncology Clinical Trials. *Ann. N.Y. Acad. Sci.* **1999**, *878*, 236−270.
(30) Jacobsen, J. A.; Fullagar, J. L.; Miller, M. T.; Cohen, S. M. Identifying chelators for metalloprotein inhibitors using a fragment-based approach. *J. Med. Chem.* **2010**, *54*, 591−602.
(31) Ropero, S.; Esteller, M. The role of histone deacetylases (HDACs) in human cancer. *Mol. Oncol.* **2007**, *1*, 19−25.
(32) Huang, B. H.; Laban, M.; Leung, C. H. W.; Lee, L.; Lee, C. K.; Salto-Tellez, M.; Raju, G. C.; Hooi, S. C. Inhibition of histone deacetylase 2 increases apoptosis and p21Cip1/WAF1 expression, independent of histone deacetylase 1. *Cell Death Differ.* **2005**, *12*, 395−404.
(33) Haggarty, S. J.; Koeller, K. M.; Wong, J. C.; Grozinger, C. M.; Schreiber, S. L. Domain-selective small-molecule inhibitor of histone deacetylase 6 (HDAC6)-mediated tubulin deacetylation. *Proc. Natl. Acad. Sci. U.S.A.* **2003**, *100*, 4389−4394.
(34) Chinchilla, R.; Najera, C. Recent advances in Sonogashira reactions. *Chem. Soc. Rev.* **2011**, *40*, 5084−5121.
(35) Chen, P. C.; Wharton, R. E.; Patel, P. A.; Oyelere, A. K. Direct diazo-transfer reaction on β-lactam: Synthesis and preliminary biological activities of 6-triazolylpenicillanic acids. *Bioorg. Med. Chem.* **2007**, *15*, 7288−7300.
(36) Gurard-Levin, Z. A.; Kilian, K. A.; Kim, J.; Bahr, K.; Mrksich, M. Peptide arrays identify isoform-selective substrates for profiling endogenous lysine deacetylase activity. *ACS Chem. Biol.* **2010**, *5*, 863−873.
(37) Trott, O.; Olson, A. J. AutoDock Vina: Improving the speed and accuracy of docking with a new scoring function, efficient optimization, and multithreading. *J. Comput. Chem.* **2010**, *31*, 455−461.
(38) Gryder, B. E.; Rood, M. K.; Johnson, K. A.; Patil, V.; Raftery, E. D.; Yao, L.-P. D.; Rice, M.; Azizi, B.; Doyle, D. F.; Oyelere, A. K. Histone deacetylase inhibitors equipped with estrogen receptor modulation activity. *J. Med. Chem.* **2013**, *56*, 5782−5796.
(39) Day, J. A.; Cohen, S. M. Investigating the selectivity of metalloenzyme inhibitors. *J. Med. Chem.* **2013**, *56*, 7997−8007.